Supporting information

2′-*O*-methylation can increase the abundance and lifetime of alternative RNA conformational states

Hala Abou Assi,[1,2] Atul K. Rangadurai,[1] Honglue Shi,[3] Bei Liu,[1] Mary C. Clay,[1] Kevin Erharter,[4] Christoph Kreutz,[4] Christopher L. Holley,[2*] and Hashim M. Al-Hashimi[1,3*]

[1]Department of Biochemistry, Duke University School of Medicine, Durham, NC 27710, USA
[2]Department of Medicine, Duke University School of Medicine, Durham, NC 27710, USA
[3]Department of Chemistry, Duke University, Durham, NC 27708, USA
[4]Institute of Organic Chemistry and Center for Molecular Biosciences Innsbruck (CMBI), University of Innsbruck, 6020 Innsbruck, Austria

* To whom correspondence should be addressed. Tel: +1 919 668 2688; Fax: +1 919 613 2321; Email: cholley@duke.edu and Tel: +1 919 660 1113; Fax: +1 919 684 8885; Email: hashim.al.hashimi@duke.edu
Present Address: Mary C. Clay, Department of Structural Biology, St. Jude Children's Research Hospital, Memphis, TN, USA

Supplementary Figures

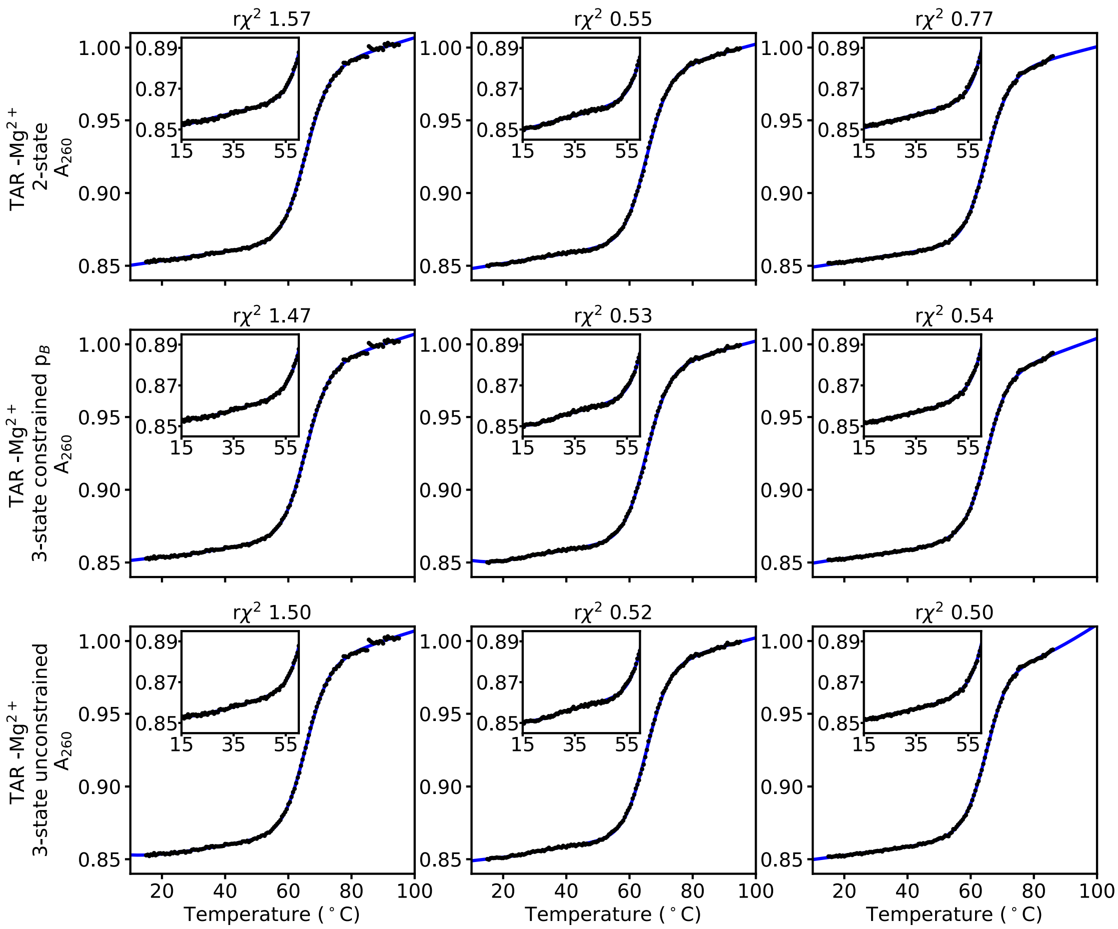

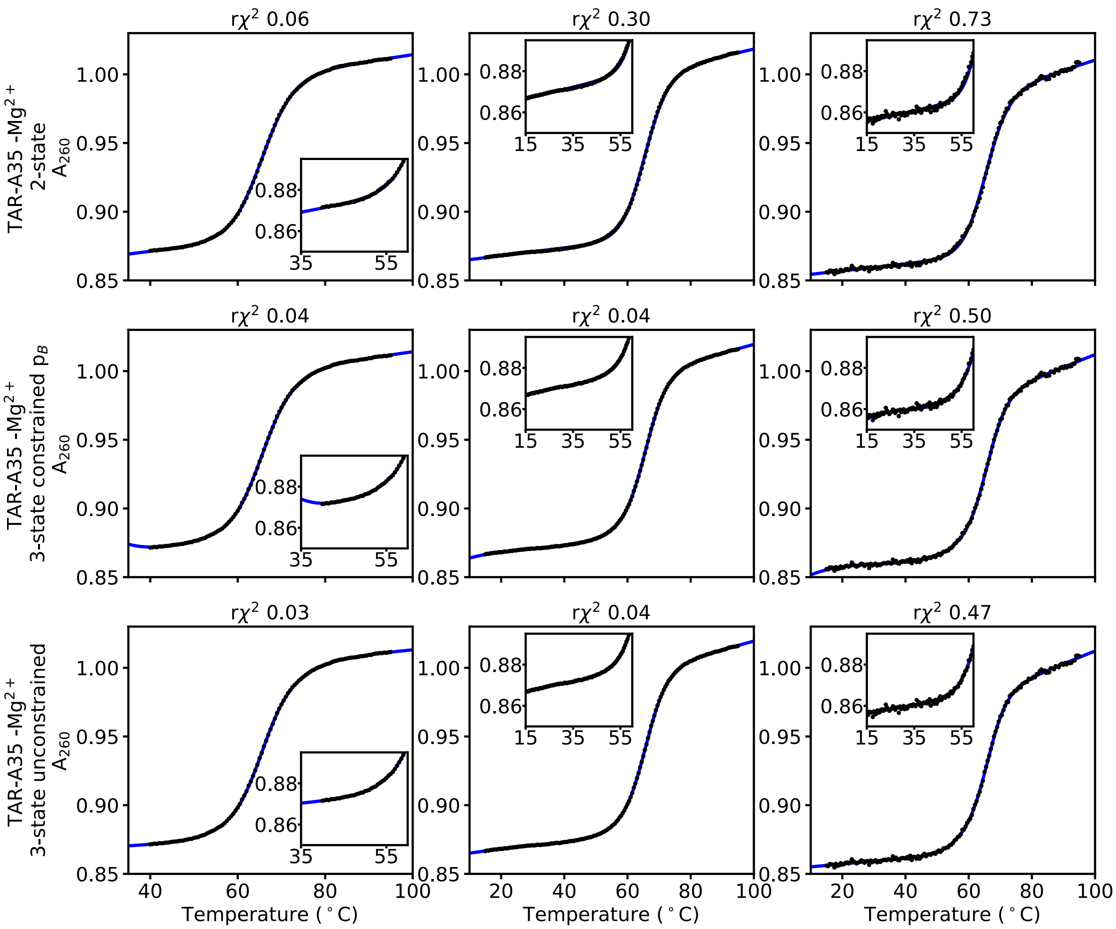

rχ2 0.06
rχ2 0.30
rχ2 0.73
rχ2 0.04
rχ2 0.04
rχ2 0.50
rχ2 0.03
rχ2 0.04
rχ2 0.47
TAR-A35 -Mg2+
2-state
A260
TAR-A35 -Mg2+
3-state constrained pB
A260
TAR-A35 -Mg2+
3-state unconstrained
A260
0.85
0.90
0.95
1.00
0.86
0.88
35
55
15
40
60
80
100
20
Temperature (°C)

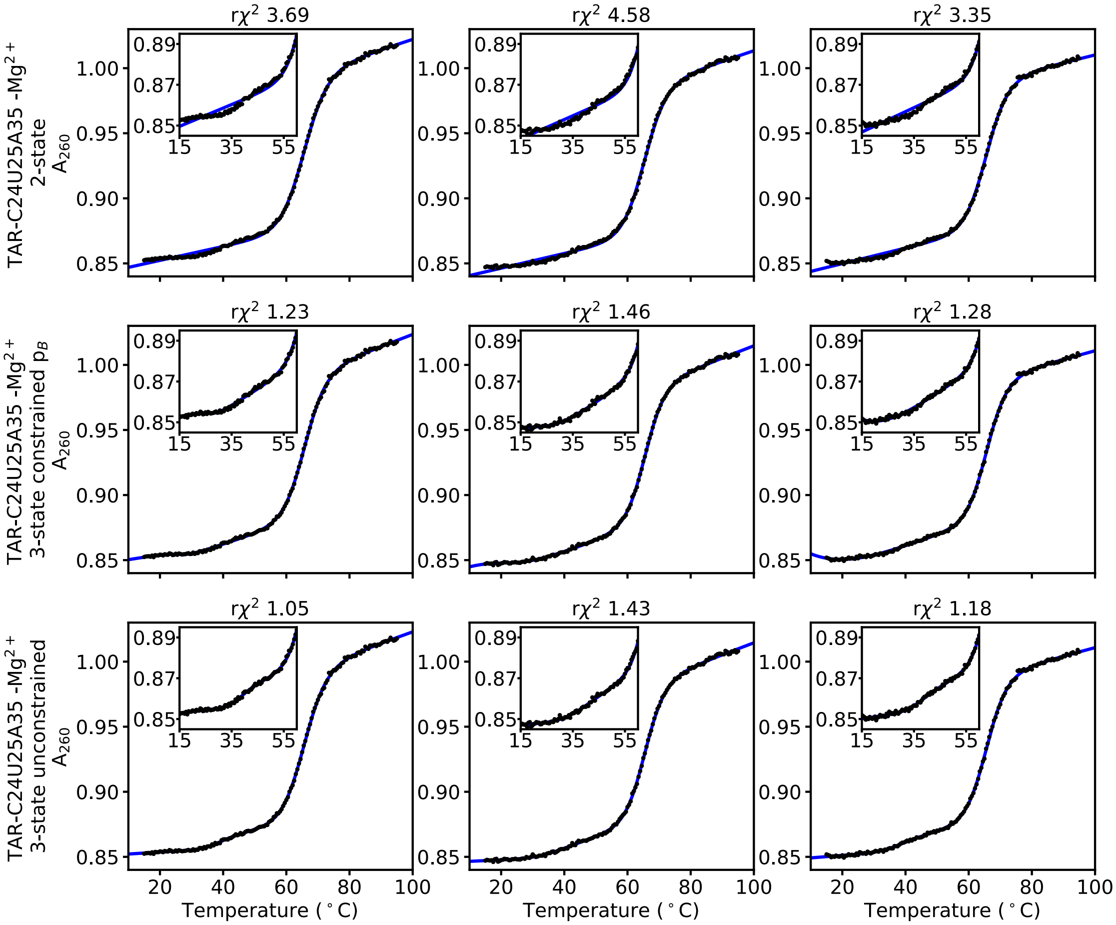

rχ^2 3.69
rχ^2 4.58
rχ^2 3.35
rχ^2 1.23
rχ^2 1.46
rχ^2 1.28
rχ^2 1.05
rχ^2 1.43
rχ^2 1.18
TAR-C24U25A35 -Mg^{2+} 2-state A$_{260}$
TAR-C24U25A35 -Mg^{2+} 3-state constrained p$_B$ A$_{260}$
TAR-C24U25A35 -Mg^{2+} 3-state unconstrained A$_{260}$
Temperature (°C)

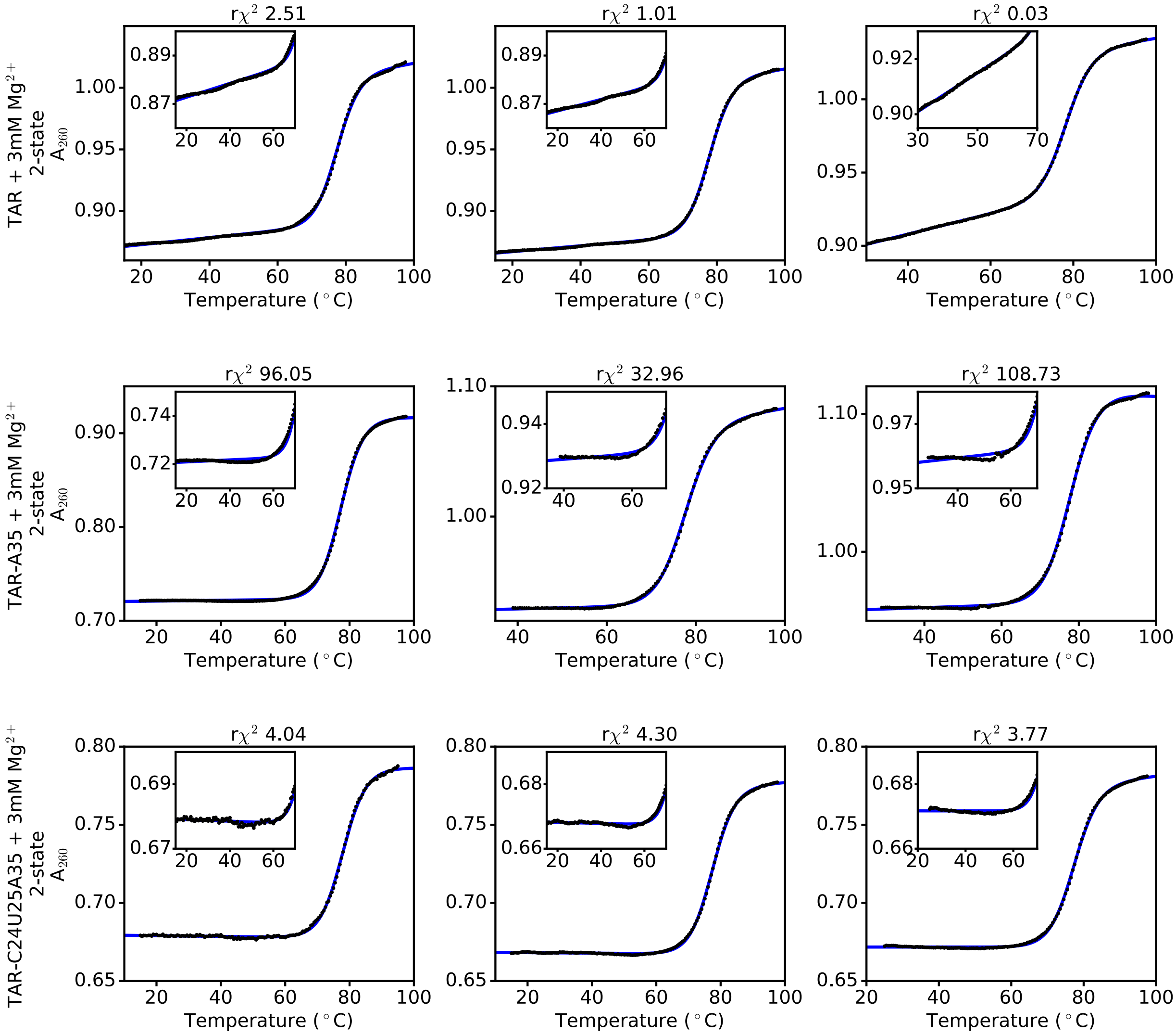

Figure S1. Fits of UV-melting data for TAR samples. Shown are the UV melting curves (black dots) for TAR variants (triplicates for each sample) and fits (blue line) to two-state, unconstrained three-state, and constrained three-state fits (see methods).

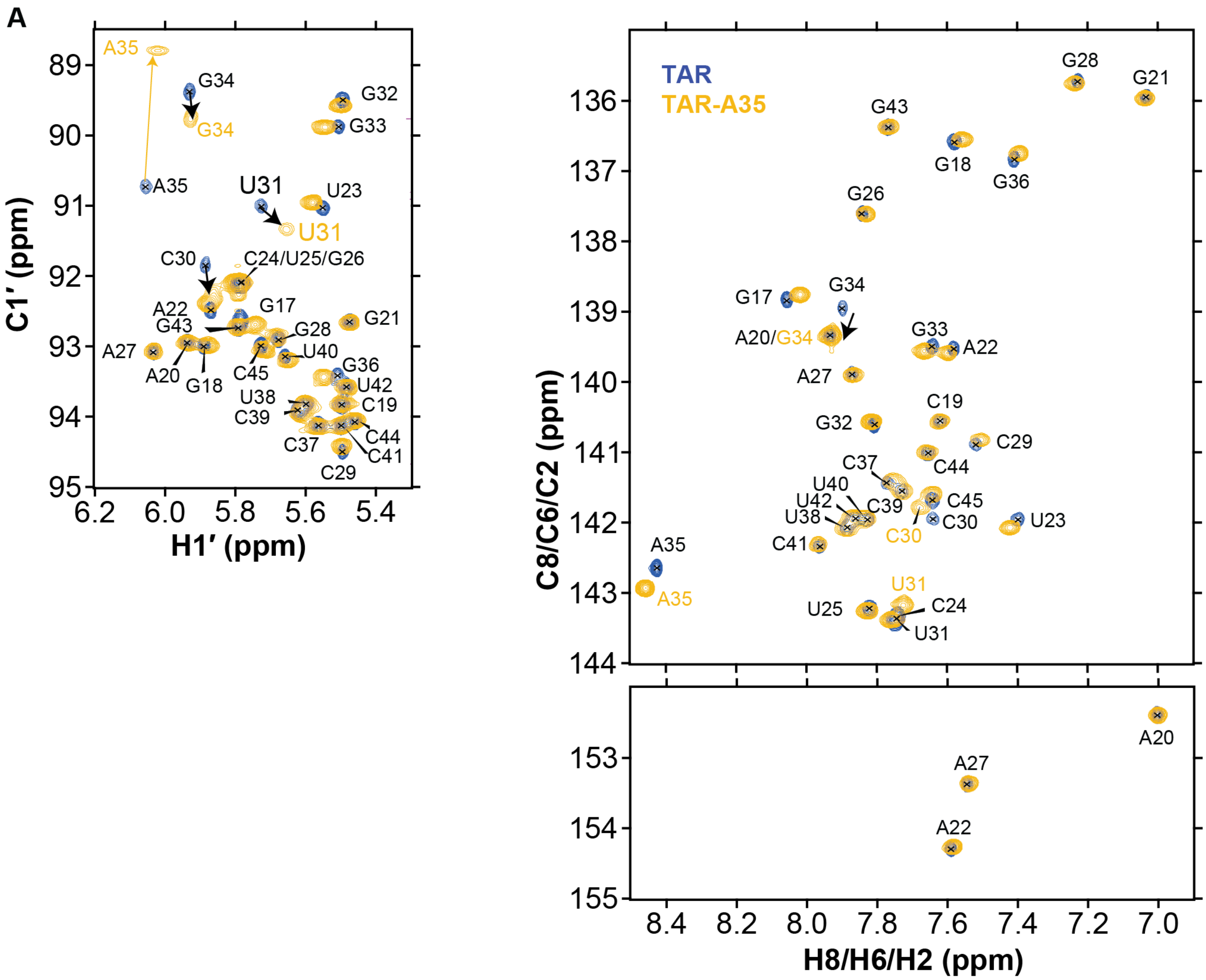

A
TAR
TAR-A35
C1′ (ppm)
H1′ (ppm)
C8/C6/C2 (ppm)
H8/H6/H2 (ppm)
A35
G34
G32
G33
U31
U23
C30
C24/U25/G26
A22
G43
G17
G28
G21
A27
A20
G18
C45
U40
G36
U42
U38
C19
C39
C37
C44
C41
C29
G28
G21
G43
G18
G36
G26
G17
A20/G34
A27
G32
C37
U40
U42
U38
C39
C41
C45
C30
U25
C24
G33
A22
C19
C29
C44
U23

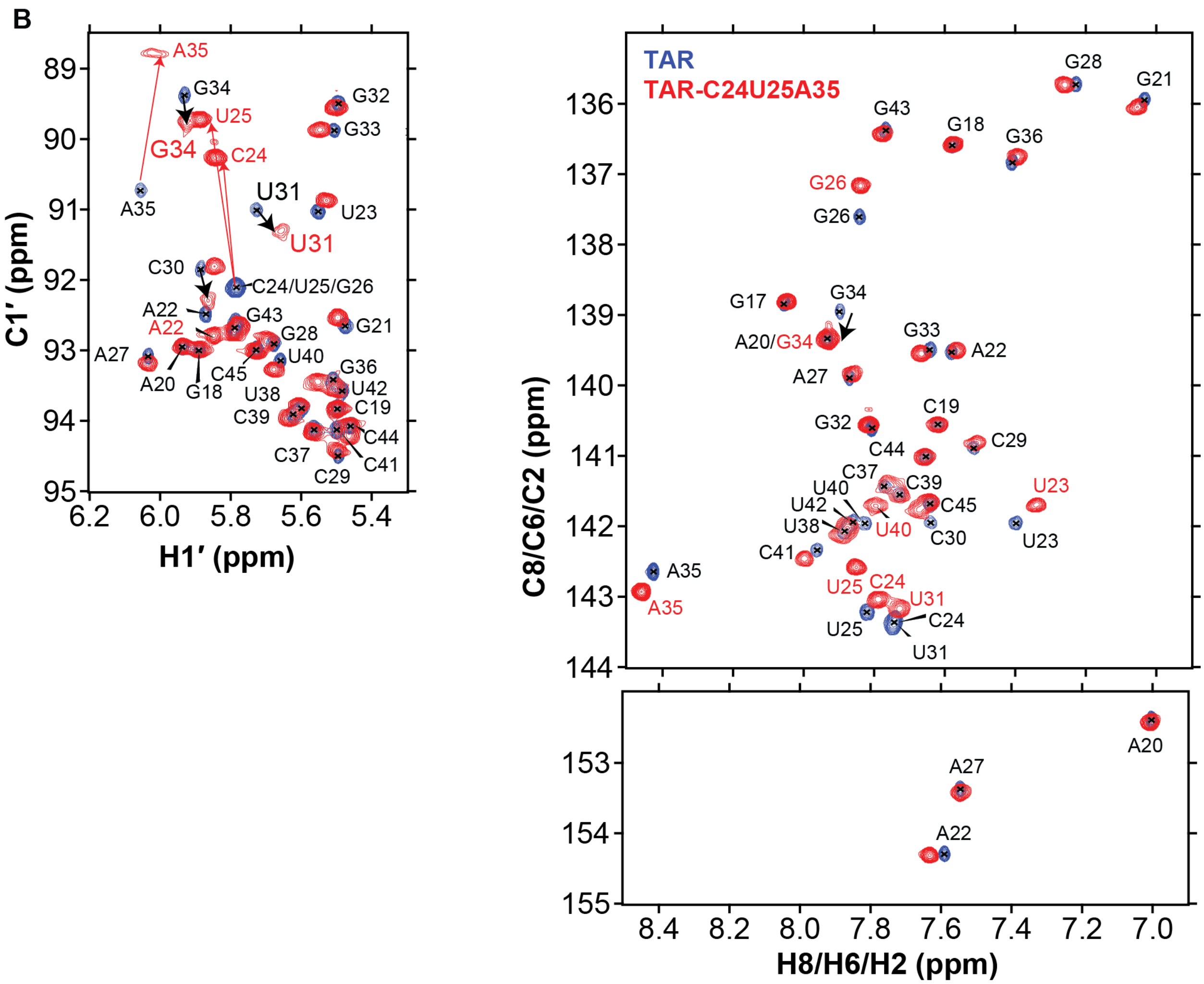

Figure S2. Overlay of unlabeled 2D [^{13}C, ^{1}H] HSQC spectra of A) TAR-A35 (pH 6.4) and B) TAR-C24U25A35 (pH 6.4) with TAR (pH 6.4). Black arrows for the C30-C1′, U31-C1′, G34-C1′ and G34-C8 indicate CSPs towards ES1 in TAR-A35 and TAR-C24U25A35. Yellow arrow at A35-C1′ in TAR-A35 and red arrows at C24-C1′, U25-C1′ and A35-C1′ in TAR-C24U25A35 indicate the upfield shift of C1′ due to the chemical modification at the 2′ position. Sample conditions: 15 mM $NaPO_4$, 25 mM NaCl and 0.1 mM EDTA, pH 6.4, and 25 ºC.

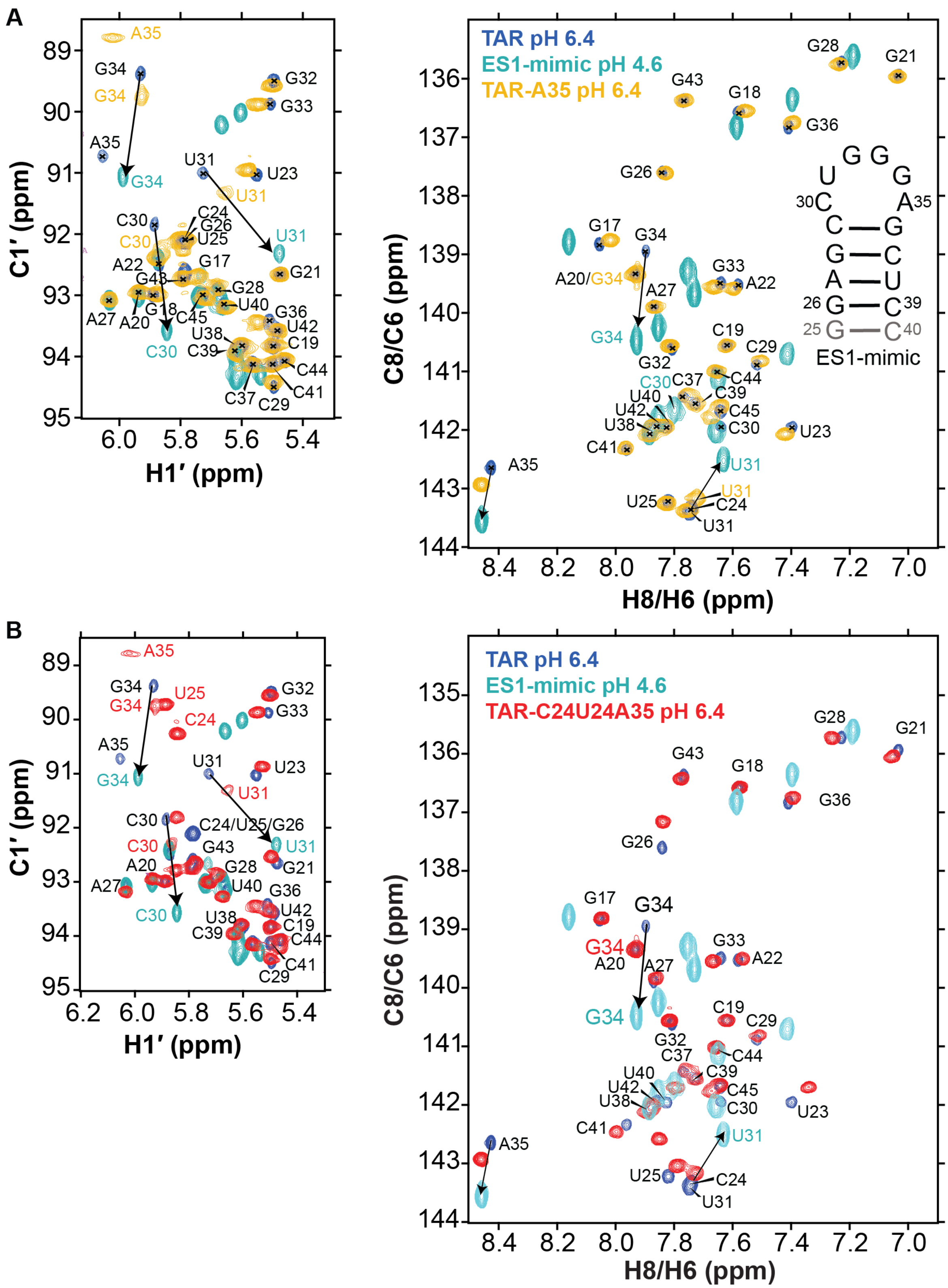

Figure S3. Overlay of C1′-H1′ and aromatic region of unlabeled 2D [^{13}C, ^{1}H] HSQC spectra of TAR (pH 6.4) and a TAR ES1-mimic (pH 4.6) (1) with A) TAR-A35 (pH 6.4) and B) TAR-C24U25A35 (pH 6.4). In the previously reported TAR ES1-mimic (1), the bulge and lower helix were omitted to simplify analysis of ES1. Black arrows at C30-C1′, U31-C1′, G34-C1′ and G34-C8 indicate a shift towards ES1 chemical shifts in TAR-A35 and TAR-C24U25A35. Sample conditions: 15 mM $NaPO_4$, 25 mM NaCl and 0.1 mM EDTA, pH 6.4, and 25 °C.

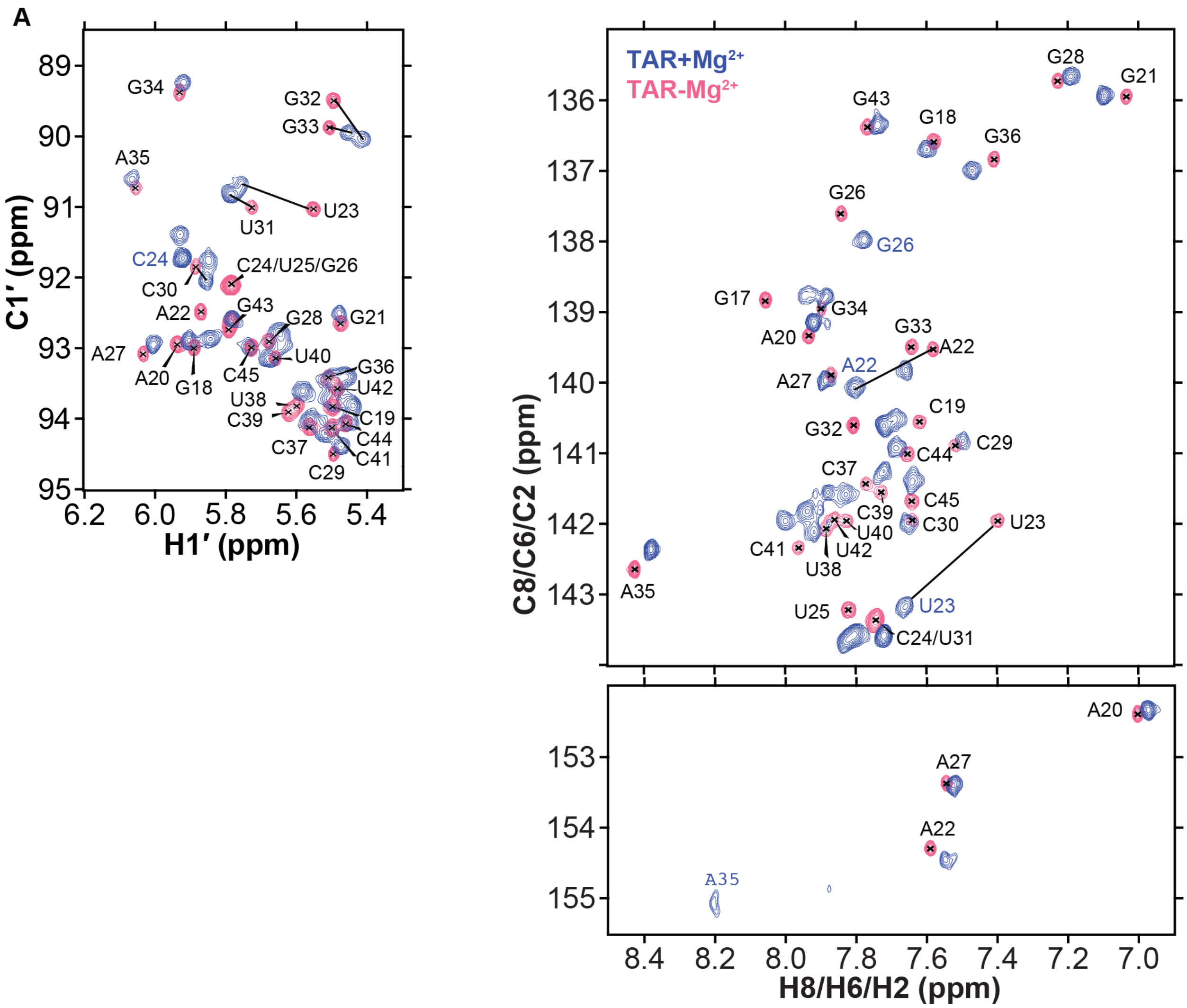

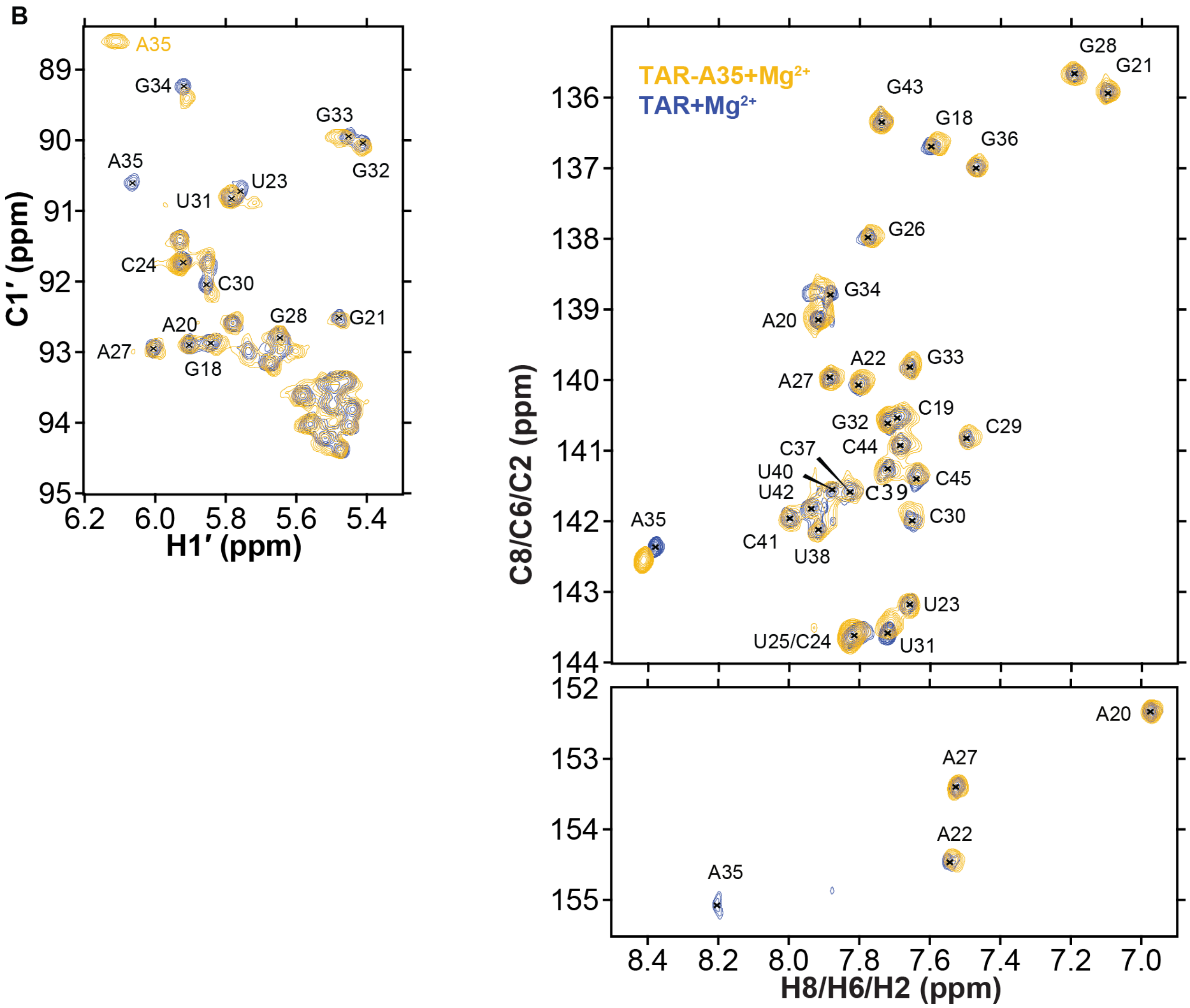
B
A35
G34
G33
G32
A35
U23
U31
C24
C30
A20
G28
G21
A27
G18
C1′ (ppm)
H1′ (ppm)
TAR-A35+Mg2+
TAR+Mg2+
G28
G21
G43
G18
G36
G26
G34
A20
A22
G33
A27
C19
G32
C29
C37
C44
U40
C45
U42
C39
A35
C30
C41
U38
U23
U25/C24
U31
A20
A27
A22
A35
C8/C6/C2 (ppm)
H8/H6/H2 (ppm)

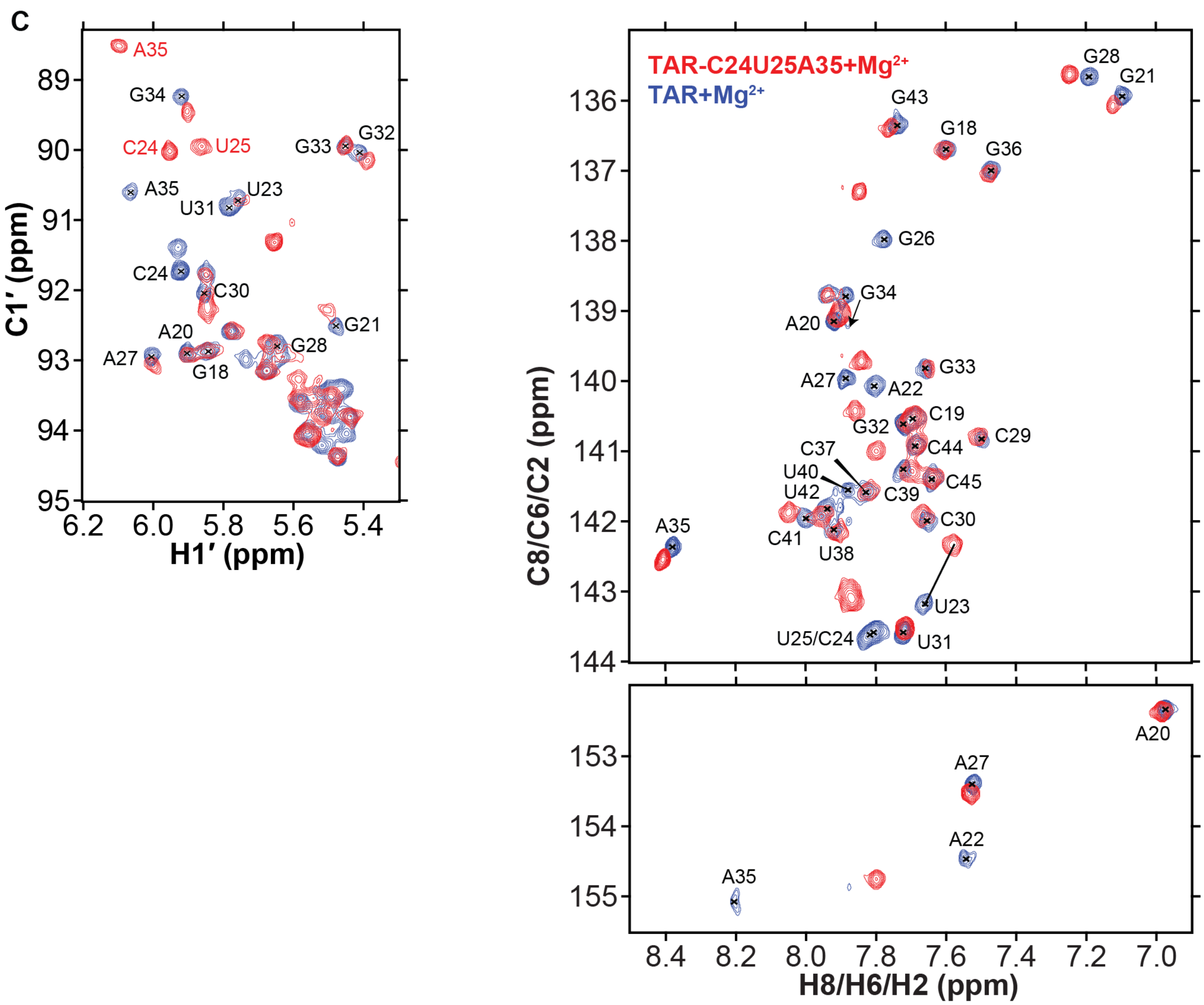

C
A35
89
G34
90
C24
U25
G33
G32
A35
U23
U31
91
C24
C30
92
G21
A20
G28
A27
93
G18
94
95
6.2
6.0
5.8
5.6
5.4
C1′ (ppm)
H1′ (ppm)
TAR-C24U25A35+Mg2+
TAR+Mg2+
G28
G21
136
G43
G18
G36
137
138
G26
G34
139
A20
G33
140
A27
A22
C19
G32
C29
141
C37
C44
U40
C45
U42
C39
142
C30
A35
C41
U38
143
U23
U25/C24
U31
144
A20
153
A27
154
A22
A35
155
8.4
8.2
8.0
7.8
7.6
7.4
7.2
7.0
C8/C6/C2 (ppm)
H8/H6/H2 (ppm)

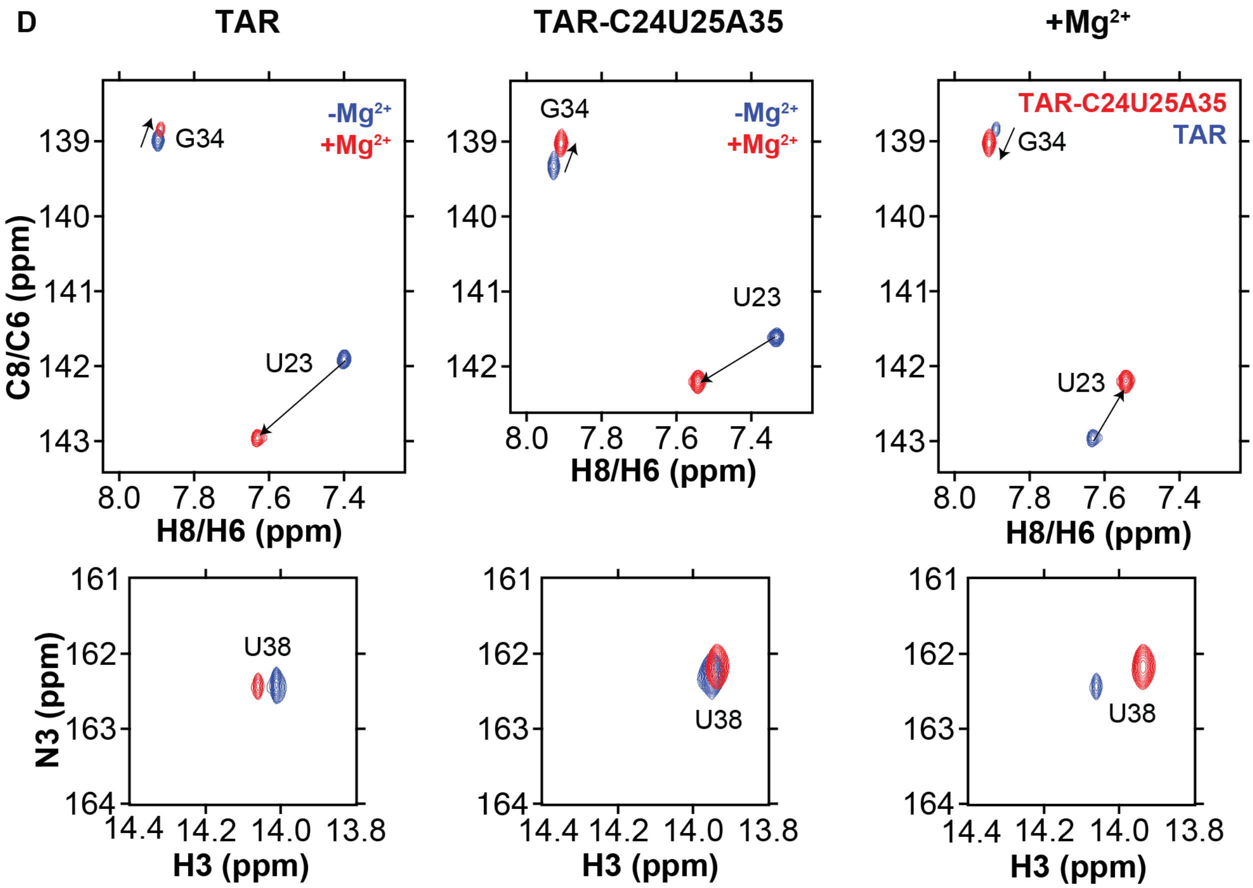

Figure S4. Overlay of unlabeled C1′-H1′ and aromatic region of 2D [^{13}C, ^{1}H] HSQC spectra of TAR (pH 6.4) in the presence of 3 mM Mg^{2+} with A) TAR (pH 6.4) in the absence of Mg^{2+}, B) TAR-A35 (pH 6.4) in 3 mM Mg^{2+} and C) TAR-C24U25A35 (pH 6.4) in 3 mM Mg^{2+}. D) Overlay of site-labeled 2D [^{13}C, ^{1}H] and 2D [^{15}N, ^{1}H] of TAR (pH 6.4) and TAR-C24U25A35 (pH 6.4) in the presence and absence of 1 mM Mg^{2+}. Samples were isotopically site-labeled with ^{13}C at G34-C8 and U23-C6 and ^{15}N at U38-N3. Sample conditions: 15 mM $NaPO_4$, 25 mM NaCl and 0.1 mM EDTA, pH 6.4, and 25 °C.

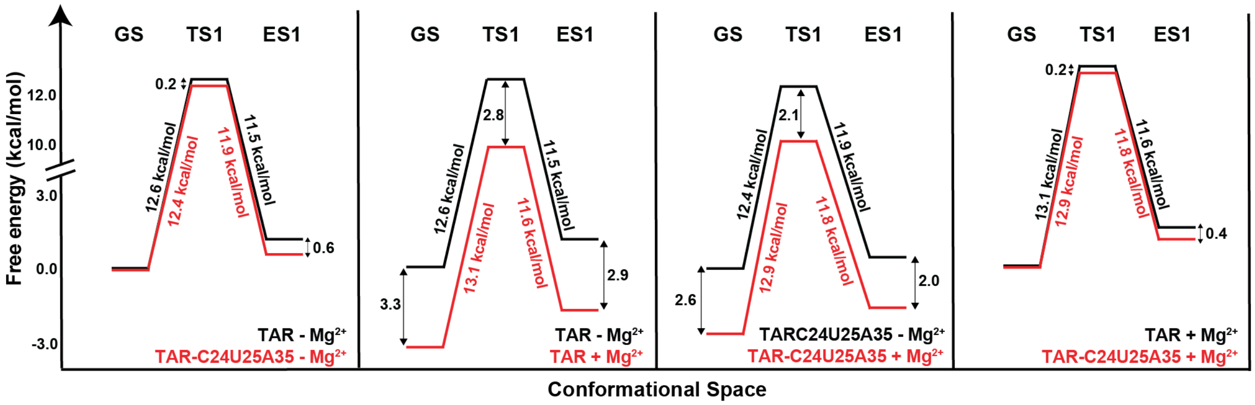

Figure S5. Free energy diagrams of GS-ES1 exchange.

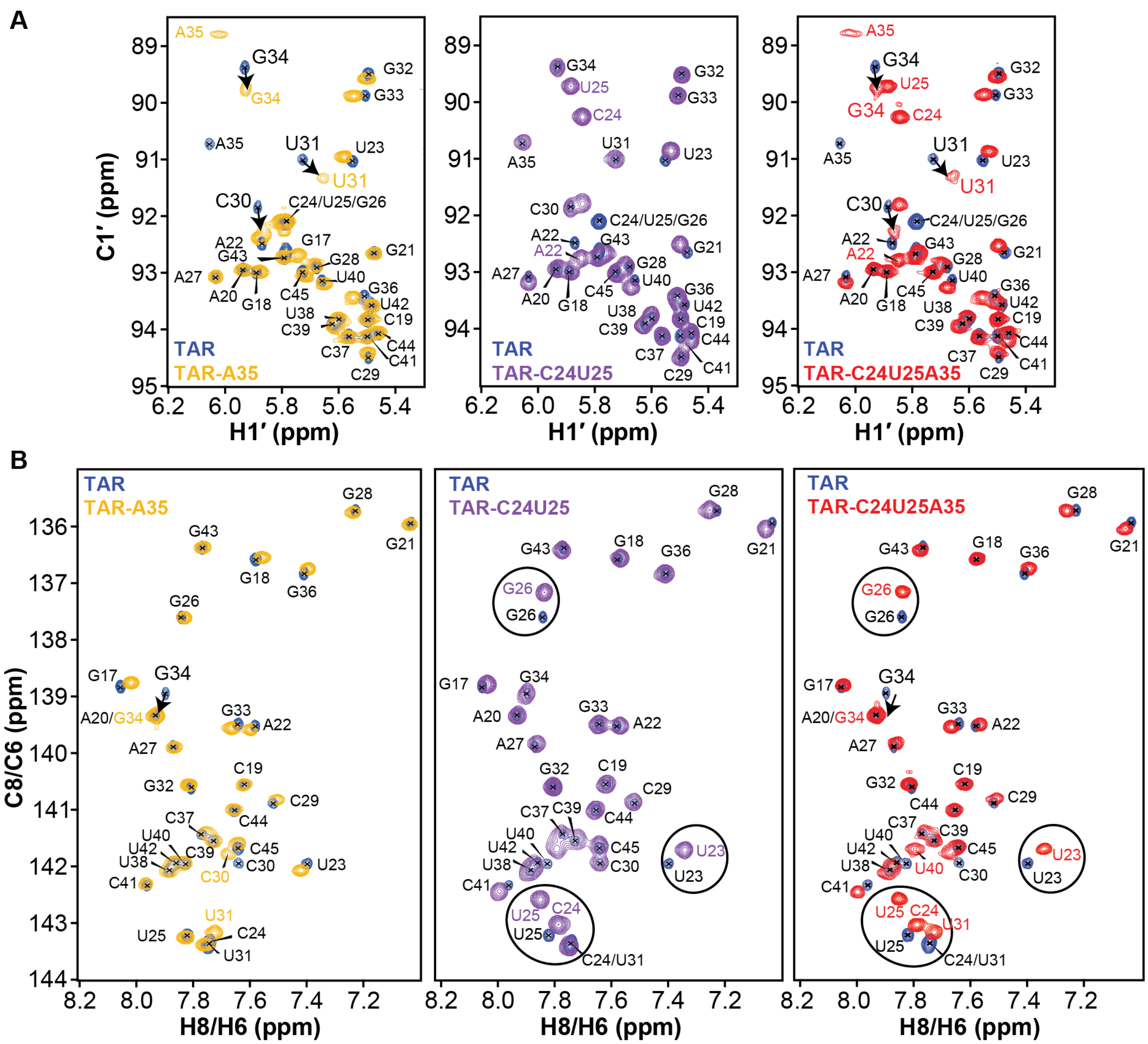

Figure S6. Overlay of A) C1′-H1′ and B) aromatic region of unlabeled 2D [^{13}C, ^{1}H] HSQC spectra of TAR with either TAR-A35, TAR-C24U25 or TAR-C24U25A35. Black arrows at C30-C1′, U31-C1′, G34-C1′ and G34-C8 in TAR-A35 and TAR-C24U25A35 indicate a shift towards ES1. Black circles around U23-C6, C24-C6, U25-C6 and G26-C8 in TAR-C24U25 or TAR-C24U25A35 indicate a shift in the GS ensemble towards the kinked conformation. Sample conditions: 15 mM $NaPO_4$, 25 mM NaCl and 0.1 mM EDTA, pH 6.4, and 25 °C.

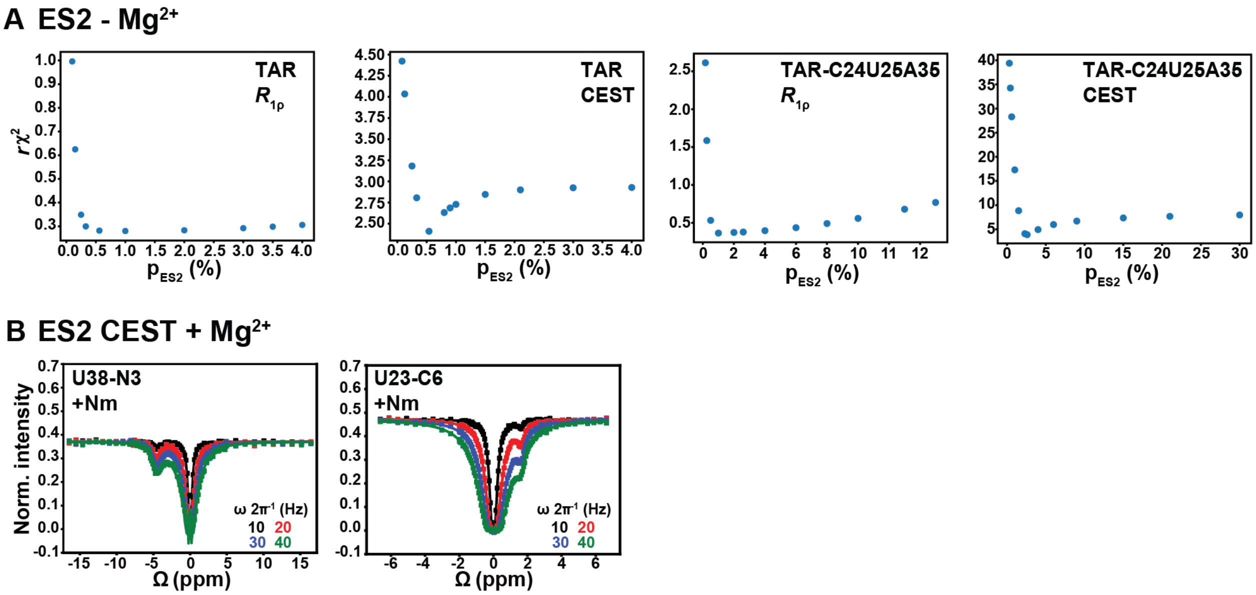

Figure S7. Supplementary $R_{1\rho}$ and CEST data for ES2. A) Uncertainty in exchange parameters obtained from fitting the $R_{1\rho}$ and CEST data. Shown are plots of reduced χ^2 ($r\chi^2$) as a function of fixing the population of ES2 to different values for TAR and TAR-C24U25A35 in the absence of Mg^{2+}. B) ^{15}N and ^{13}C CEST profiles for U23-C6 and U38-N3 for TAR-C24U25A35 (pH 6.4) at 25°C in the presence of 1 mM Mg^{2+}. $\Omega = \omega_{RF}-\omega_{OBS}$. Spin-lock powers are color-coded.

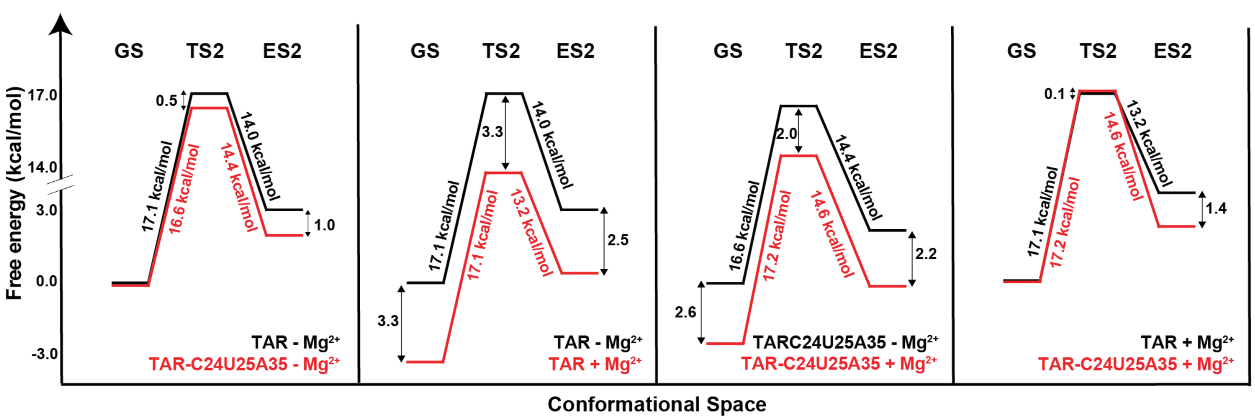

Figure S8. Free energy diagrams of GS-ES2 exchange.

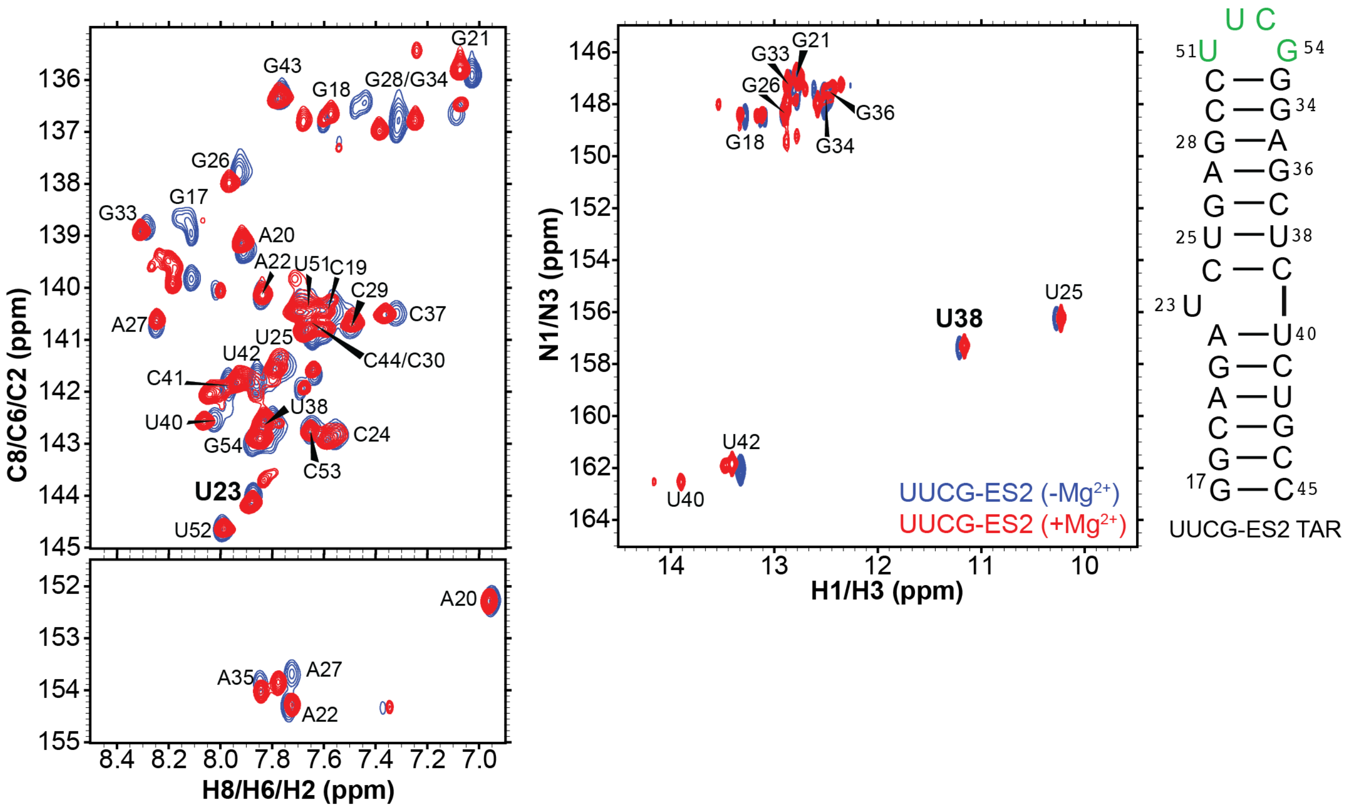

Figure S9. The effect of Mg^{2+} on the chemical shifts of ES2 probes. Overlay of uniformly $^{13}C/^{15}N$ labeled [^{13}C,^{1}H] and [^{15}N,^{1}H] 2D HSQC spectra of UUCG-ES2 mutant (3) in the presence and absence of 1 mM Mg^{2+}. UUCG-ES2 stabilizes ES2 (3) as the dominant conformation through replacement of the native TAR apical loop with a UUCG loop. The addition of 1 mM Mg^{2+} does not significantly affect the chemical shifts of the ES2 probes (U23-C6 and U38-N3) used in this study. Sample conditions: 15 mM $NaPO_4$, 25 mM NaCl and 0.1 mM EDTA, pH 6.4, and 25 °C.

Tables

Table S1. Thermodynamic parameters obtained from two-state fitting (in the presence and absence of Mg^{2+}), as well as unconstrained and constrained three-state fitting (in the absence of Mg^{2+}) of the UV melting data measured for TAR samples.

	Two-state fitting							
	No Mg^{2+}				+ 3 mM Mg^{2+}			
Sample	T_m (°C)	ΔH^{o}_{melt} (kcal/mol)	$T\Delta S^{o}_{melt}$ (kcal/mol)	$\Delta G^{o}_{melt,37C}$ (kcal/mol)	T_m (°C)	ΔH^{o}_{melt} (kcal/mol)	$T\Delta S^{o}_{melt}$ (kcal/mol)	$\Delta G^{o}_{melt,37C}$ (kcal/mol)
TAR	65.2±0.2	-62.8±1.1	-57.5±1.0	-5.2±0.1	77.8±0.4	-75.1±2.8	-66.4±2.4	-8.7±0.4
TAR-A35	65.4±0.2	-63.0±0.9	-57.7±0.8	-5.3±0.1	77.6±0.2	-71.7±2.2	-63.4±1.8	-8.3±0.2
TAR-C24U25A35	65.5±0.1	-65.0±2.4	-59.5±2.2	-5.5±0.2	77.5±0.3	-70.0±1.6	-61.9±1.4	-8.1±0.1
No Mg^{2+}								
Unconstrained three-state fitting								
Sample	ΔH^{o}_{melt} (kcal/mol)	$T\Delta S^{o}_{melt}$ (kcal/mol)	$\Delta G^{o}_{melt,37C}$ (kcal/mol)	ΔH^{o}_{conf} (kcal/mol)	$T\Delta S^{o}_{conf}$ (kcal/mol)	$\Delta G^{o}_{conf,37C}$ (kcal/mol)		
TAR	-98.2±47.6	-93.9±49.3	-4.3±1.7	45.1±44.4	43.1±46.9	2.0±4.7		
TAR-A35	-99.1±15.3	-91.4±14.3	-7.7±1.1	37.5±12.7	34.9±11.6	2.6±1.3		
TAR-C24U25A35	-123.9±11.5	-118.1±11.6	-5.8±0.1	54.6±14.5	54.6±14.4	0.003±0.2		
Constrained three-state fitting								
TAR (13%)	-65.6±3.8	-60.2±3.6	-5.4±0.2	-51.5±49.6	-54.7±51.6	3.2±2.0		
TAR-A35 (30%)	-71.0±2.5	-65.4±2.2	-5.5±0.3	5.1±0.8	4.7±0.8	0.3±0.03		
TAR-C24U25A35 (30%)	-97.8±35.5	-92.9±36.9	-5.1±1.4	15.2±47.6	15.3±49.5	-0.1±1.9		

ΔH^{o}_{melt}, ΔH^{o}_{conf}, ΔS^{o}_{melt}, ΔS^{o}_{conf} refer to the enthalpies and entropies of the annealing and conformational change, $\Delta G^{o}_{melt,37C}$ and $\Delta G^{o}_{conf,37C}$ are the free energies of melting and conformational change respectively, at 37 °C and T is the temperature in Kelvin. For the constrained three-state fit, ΔG^{o}_{conf} was constrained such that the population of the conformational change was equal to that obtained from $R_{1\rho}$ measurements at 25 °C (Table S5, 13% for TAR and 30% for TAR-A35 and TAR-C24U25A35 in the absence of Mg^{2+}). The population of ES1 at 25 °C in TAR-A35 was assumed to be the same as that measured by $R_{1\rho}$ on TAR-C24U25A35 at 25 °C. Errors were defined as the standard deviation of the respective parameters obtained from triplicate measurements. Buffer conditions are 15 mM $NaPO_4$, 25 mM NaCl and 0.1 mM EDTA, with and without 3 mM Mg^{2+}.

Table S2. Comparison of thermodynamic parameters obtained from two-state and unconstrained three-state fitting of the UV melting data for TAR samples in the absence of Mg^{2+}.

Sample	$\Delta G^{o}_{melt,25C}$ (two-state) (kcal/mol)	$\Delta G^{o}_{melt,25C}$ (unconstrained three-state) (kcal/mol)	$\Delta G^{o}_{conf,25C}$ (unconstrained three-state) (kcal/mol)	$\Delta G^{o}_{conf,25C}$ ($R_{1\rho}$) (kcal/mol)	Significant fit
TAR	-7.5±0.1	-7.9±0.4	3.7±4.0	1.1	2/3-state free*
TAR-C24U25A35	-7.8±0.3	-10.4±0.3	2.1±0.7	0.5	3-state free

$\Delta G^{o}_{melt,25C}$ and $\Delta G^{o}_{conf,25C}$ denote the free energy of annealing and the conformational change at 25°C, respectively. *Some of the individual melts of the triplicate set of measurements fit better to a 2-state and the others to a 3-state free fit based on AIC/BIC statistical criteria.

Table S3. Perturbations in chemical shifts of A and U upon 2′-*O*-methylation computed using density functional theory (DFT) calculations.

Entry		A-C8	A-C2	A-C1'	A-C2'	A-C3'	A-C4'	U-C6	U-C1'	U-C2'	U-C3'	U-C4'
1	rA C3'-endo	142.56	156.21	95.316	78.8973	70.1277	85.4643					
2	rU C3'-endo							147.234	93.9691	77.7646	69.8541	85.629
3	rA C2'-endo	140.01	157.01	94.465	75.158	77.4695	89.7878					
4	rU C2'-endo							145.029	94.6564	74.5493	78.1384	88.483
5	Am, C3'-endo	142.71	155.96	92.459	90.5046	70.39	85.9056					
6	Um, C3'-endo							146.916	91.3198	89.5421	70.1019	86.499
7	Am, C2'-endo	140.75	156.66	92.608	83.1558	77.2877	89.109					
8	Um, C2'-endo							145.555	93.7743	82.5949	77.1266	88.861

Table S4. Population of ES1 derived from chemical shift perturbation analysis.

	Shift toward ES1 (%)			
	$-Mg^{2+}$		+1 mM Mg^{2+}	
Resonance	TAR-A35	TAR-C24U24A35	TAR	TAR-C24U24A35
C30C1′-H1′	30.5	34.1		
U31C1′-H1′	28.7	27.1		
U31C6-H6	27.5	27.7		
G34C1′-H1′	29.7	29.2		
G34C8-H8	27.0	26.1	7.3	14.5
Average	28.7	28.8		
STDEV	1.5	3.1		

Table S5. Exchange parameters for ES1 from fitting $R_{1\rho}$ data for G34-C8 at 25 ^oC.

	R_1 (Hz)	R_2 (Hz)	p_{ES1} (%)	Δω (ppm)	k_{ex} (s^{-1})	k_1 (s^{-1})	k_{-1} (s^{-1})	τ (μs)	ΔG° (kcal/mol)
1) TAR -Mg^{2+} from (1)	2.3 ± 0.1	22.3 ± 1.2	13.0 ± 2.0	2.6 ± 0.2	25807 ± 716	3436 ± 509	22371 ± 1771	45 ± 4	1.1 ± 0.1
2) TAR -Mg^{2+}	3.4 ± 0.3	28.9 ± 5.6	21.9 ± 10.0	2.6 ± 0.5	32248 ± 4214	7055 ± 2839	25193 ± 4248	40 ± 7	0.75 ± 0.3
3) TAR -Mg^{2+}	3.3 ± 0.2	31.3 ± 4.4	13*	3.0 ± 0.4	30531 ± 3484	3969 ± 3521	26562 ± 4624	38 ± 7	1.1
4) TAR-C24U25A35 -Mg^{2+}	1.2 ± 0.4	32.6 ± 2.1	30.3 ± 6.0	2.4 ± 0.2	15874 ± 613	4816 ± 752	11059 ± 848	90 ± 7	0.5 ± 0.1
5) TAR-C24U25A35 -Mg^{2+}	1.2 ± 0.4	32.7 ± 2.1	29**	2.4 ± 0.1	15852 ± 613	4597 ± 3530	11255 ± 3553	89 ± 28	0.5**
6) TAR +1 mM Mg^{2+}	2.6 ± 0.2	37.3 ± 2.6	7.0**	2.9 ± 0.3	23516 ± 2685	1646 ± 1547	21870 ± 2932	46 ± 6	1.5**
7) TAR-C24U25A35 +1 mM Mg^{2+}	2.1 ± 0.2	37.2 ± 1.1	14.1 ± 2.8	2.5 ± 0.2	15098 ± 487	2122 ± 372	12976 ± 556	77 ± 3	1.1 ± 0.1

*values fixed while fitting the data, these values are obtained from previously published results (1)

**p_{ES1} from chemical shift perturbation analysis in 2D HSQC NMR and the corresponding ΔG° is calculated based on the following equation: $RT\ln[p_{ES1}/(1-p_{ES1})]$

Table S6. Free energy values calculated for TS1 and TS2.

ES	Condition	$\Delta^{\ddagger}G^o$ kcal/mol
ES1	TAR	12.6 ± 0.1
	TAR-C24U25A35	12.4 ± 0.1
	TAR + Mg^{2+}	13.1 ± 0.6
	TAR-C24U25A35 + Mg^{2+}	12.9 ± 0.1
ES2	TAR	17.06 ± 0.04
	TAR-C24U25A35	16.56 ± 0.01
	TAR + Mg^{2+}	17.06 ± 0.14
	TAR-C24U25A35 + Mg^{2+}	17.15 ± 0.03

Table S7. Phi-values for Nm-modified TAR in the absence and presence of Mg^{2+}.

ES	Sample	Φ
ES1	TAR-C24U25A35	0.33 ± 0.25
	TAR-C24U25A35 + Mg^{2+}	0.5 ± 1.6*
ES2	TAR-C24U25A35	0.53 ± 0.04
	TAR-C24U25A35 + Mg^{2+}	-0.07 ± 0.10*

*Phi-value calculated for TAR-C24U25A35 in the presence of Mg^{2+} with TAR in Mg^{2+} as a reference.

Table S8A. Comparison of ES2 exchange parameters for TAR and TAR-C24U25A35 obtained from fitting CEST and $R_{1\rho}$ data in the absence of Mg^{2+}.

	R1 (Hz)	R2 (Hz)	p_{ES2} (%)	Δω (ppm)	k_{ex} (s^{-1})	k_1 (s^{-1})	k_{-1} (s^{-1})	τ (ms)	ΔG° (kcal/mol)
TAR U23-C6 from (3)	2.50 ± 0.04	30.7 ± 0.1	0.40 ± 0.05	2.3 ± 0.1	474 ± 69	1.9 ± 0.4	472 ± 70	2.1 ± 0.3	3.26 ± 0.07
TAR U38-N3 from (3)	1.40 ± 0.03	6.20 ± 0.03		-5.2 ± 0.2					
TAR CEST (U23-C6)	2.702 ± 0.004	30.38 ± 0.19	0.54 ± 0.01	2.07 ± 0.02	356 ± 23	1.92 ± 0.13	354 ± 23	2.8 ± 0.2	3.09 ± 0.01
TAR CEST (U38-N3)	3.111 ± 0.005	9.90 ± 0.13		-5.12 ± 0.06					
TAR RD (U23-C6)	2.71 ± 0.07	30.07 ± 0.09	0.54*	2.32 ± 0.13	431 ± 15	2.3 ± 2.3	429 ± 15	2.33 ± 0.08	
TAR RD (U38-N3)	2.03 ± 0.02	6.29 ± 0.02		-4.89 ± 0.13					
TAR-C24U25A35 CEST (U23-C6)	2.538 ± 0.003	31.15 ± 0.14	2.60 ± 0.03	2.142 ± 0.003	171 ± 3	4.45 ± 0.09	167 ± 3	6.0 ± 0.1	2.15 ± 0.01
TAR-C24U25A35 CEST (U38-N3)	3.458 ± 0.004	10.21 ± 0.08		-4.877 ± 0.009					
TAR-C24U25A35 RD (U23-C6)	2.9 ± 0.1	33.53 ± 0.13	2.6*	2.25 ± 0.08	174 ± 5	4.5 ± 4.4	170 ± 6	5.9 ± 0.2	
TAR-C24U25A35 RD (U38-N3)	2.15 ± 0.03	6.68 ± 0.03		-4.56 ± 0.09					

* $R_{1\rho}$ RD data was fit by fixing the population to the values determined by CEST.

Table S8B. Comparison of ES2 exchange parameters for TAR and TAR-C24U25A35 in the presence of 1 mM Mg^{2+} obtained from fitting CEST and $R_{1\rho}$ data.

	R1 (Hz)	R2 (Hz)	p_{ES2} (%)	Δω (ppm)	k_{ex} (s^{-1})	k_1 (s^{-1})	k_{-1} (s^{-1})	τ (ms)	ΔG° (kcal/mol)
TAR RD (U38-N3)	2.02 ± 0.03	6.62 ± 0.05	0.14 ± 0.02	-4.4 ± 0.5	1367 ± 267	1.92 ± 0.47	1365 ± 266	0.73 ± 0.14	3.89 ± 0.19
TAR-C24U25A35 CEST (U23-C6)	2.459 ± 0.003	39.25 ± 0.17	1.39 ± 0.03	1.631 ± 0.004	118 ± 4	1.65 ± 0.07	116 ± 4	8.6 ± 0.3	2.52 ± 0.01
TAR-C24U25A35 CEST (U38-N3)	3.255 ± 0.003	10.49 ± 0.07		-4.66 ± 0.01					
TAR-C24U25A35 RD (U23-C6)	2.6 ± 0.1	41.66 ± 0.13	1.4*	2.0 ± 0.2	117 ± 5	1.6 ± 1.6	116 ± 5	8.6 ± 0.4	
TAR-C24U25A35 RD (U38-N3)	1.96 ± 0.02	7.14 ± 0.02		-4.43 ± 0.15					

* $R_{1\rho}$ RD data for TAR-C24U25A35 was fit by fixing the population to the values determined by CEST.

Table S9. Spin-lock power and offsets used in the $R_{1\rho}$ measurements.

construct	Nuclei	**[spin-lock power] {offset frequencies}/[ω_1 $2\pi^{-1}$(s^{-1})] {Ω $2\pi^{-1}$(s^{-1})}**
TAR (-Mg^{2+})	U23-C6	[50, 100, 150, 200, 250, 300, 350, 400, 500, 600, 700, 800, 900, 1000, 1200, 1400, 1600, 1800, 2000, 2500] {0}
		[200] {-800, -700, -600, -540, -480, -420, -390, -360, -330, -300, -270, -240, -210, -180, -150, -120, -90, -60, -30, 30, 60, 90, 120, 150, 180, 210, 240, 270, 300, 330, 360, 390, 420, 480, 540, 600, 700, 800}
		[400] {-1500, -1200, -1000, -900, -800, -700, -600, -550, -500, -450, -400, -350, -300, -250, -200, -150, -100, -50, 50, 100, 150, 200, 250, 300, 350, 400, 450, 500, 550, 600, 700, 800, 900, 1000, 1200, 1500}
		[600] {-1600, -1400, -1200, -1000, -800, -650, -550, -450, -375, -300, -225, -150, -75, 75, 150, 225, 300, 375, 450, 550, 650, 800, 1000, 1200, 1400, 1600}
		[1000] {-1700, -1500, -1300, -1100, -900, -700, -500, -400, -300, -200, -100, 100, 200, 300, 400, 500, 700, 900, 1100, 1300, 1500, 1700}
	U38-N3	[100, 150, 200, 250, 300, 350, 400, 450, 500, 500, 600, 700, 800, 900, 1000, 1200, 1400, 1600, 1800, 2000] {0}
		[200] {-500, -400, -350, -300, -250, -225, -200, -180, -160, -140, -120, -100, -80, -60, -40, -20, 20, 40, 60, 80, 100, 120, 140, 160, 180, 200, 225, 250, 300, 350, 400, 500}
		[400] {-1000, -800, -700, -600, -500, -400, -350, -300, -250, -210, -180, -150, -120, -90, -60, -30, 30, 60, 90, 120, 150, 180, 210, 250, 300, 350, 400, 500, 600, 700, 800, 1000}
		[600] {-1600, -1400, -1200, -1000, -800, -600, -500, -400, -300, -240, -200, -160, -120, -80, -40, 40, 80, 120, 160, 200, 240, 300, 400, 500, 600, 800, 1000, 1200, 1400, 1600}
		[1000] {-3000, -2500, -2000, -1500, -1300, -1100, -900, -700, -600, -500, -400, -300, -200, -100, 100, 200, 300, 400, 500, 600, 700, 900, 1100, 1300, 1500, 2000, 2500, 3000}
TAR-C24U25A35 (-Mg^{2+})	U23-C6	[200, 250, 300, 350, 400, 500, 600, 700, 800, 900, 1000, 1200, 1400, 1600, 1800, 2000, 2500] {0}
		[200] {-800, -700, -600, -540, -480, -420, -390, -360, -330, -300, -270, -240, -210, -180, -150, -120, -90, -60, -30, 30, 60, 90, 120, 150, 180, 210, 240, 270, 300, 330, 360, 390, 420, 480, 540, 600, 700, 800}
		[400] {-1500, -1200, -1000, -900, -800, -700, -600, -550, -500, -450, -400, -350, -300, -250, -200, -150, -100, -50, 50, 100, 150, 200, 250, 300, 350, 400, 450, 500, 550, 600, 700, 800, 900, 1000, 1200, 1500}
		[600] {-1600, -1400, -1200, -1000, -800, -650, -550, -450, -375, -300, -225, -150, -75, 75, 150, 225, 300, 375, 450, 550, 650, 800, 1000, 1200, 1400, 1600}
		[1000] {-1700, -1500, -1300, -1100, -900, -700, -500, -400, -300, -200, -100, 100, 200, 300, 400, 500, 700, 900, 1100, 1300, 1500, 1700}
	U38-N3	[100, 150, 200, 250, 300, 350, 400, 450, 500, 500, 600, 700, 800, 900, 1000, 1200, 1400, 1600, 1800, 2000] {0}
		[200] {-500, -400, -350, -300, -250, -225, -200, -180, -160, -140, -120, -100, -80, -60, -40, -20, 20, 40, 60, 80, 100, 120, 140, 160, 180, 200, 225, 250, 300, 350, 400, 500}
		[400] {-1000, -800, -700, -600, -500, -400, -350, -300, -250, -210, -180, -150, -120, -90, -60, -30, 30, 60, 90, 120, 150, 180, 210, 250, 300, 350, 400, 500, 600, 700, 800, 1000}
		[600] {-1600, -1400, -1200, -1000, -800, -600, -500, -400, -300, -240, -200, -160, -120, -80, -40, 40, 80, 120, 160, 200, 240, 300, 400, 500, 600, 800, 1000, 1200, 1400, 1600}
		[1000] {-3000, -2500, -2000, -1500, -1300, -1100, -900, -700, -600, -500, -400, -300, -200, -100, 100, 200, 300, 400, 500, 600, 700, 900, 1100, 1300, 1500, 2000, 2500, 3000}
TAR (+Mg^{2+})	U38-N3	[100, 150, 200, 250, 300, 350, 400, 450, 500, 500, 600, 700, 800, 900, 1000, 1200, 1400, 1600, 1800, 2000] {0}

		[200] {-500, -400, -350, -300, -250, -225, -200, -180, -160, -140, -120, -100, -80, -60, -40, -20, 20, 40, 60, 80, 100, 120, 140, 160, 180, 200, 225, 250, 300, 350, 400, 500}
		[400] {-1000, -800, -700, -600, -500, -400, -350, -300, -250, -210, -180, -150, -120, -90, -60, -30, 30, 60, 90, 120, 150, 180, 210, 250, 300, 350, 400, 500, 600, 700, 800, 1000}
		[600] {-1600, -1400, -1200, -1000, -800, -600, -500, -400, -300, -240, -200, -160, -120, -80, -40, 40, 80, 120, 160, 200, 240, 300, 400, 500, 600, 800, 1000, 1200, 1400, 1600}
		[1000] {-3000, -2500, -2000, -1500, -1300, -1100, -900, -700, -600, -500, -400, -300, -200, -100, 100, 200, 300, 400, 500, 600, 700, 900, 1100, 1300, 1500, 2000, 2500, 3000}
TAR-C24U25A35 (+Mg^{2+})	U23-C6	[50, 100, 150, 200, 250, 300, 350, 400, 500, 600, 700, 800, 900, 1000, 1200, 1400, 1600, 1800, 2000, 2500] {0}
		[200] {-800, -700, -600, -540, -480, -420, -390, -360, -330, -300, -270, -240, -210, -180, -150, -120, -90, -60, -30, 30, 60, 90, 120, 150, 180, 210, 240, 270, 300, 330, 360, 390, 420, 480, 540, 600, 700, 800}
		[400] {-1500, -1200, -1000, -900, -800, -700, -600, -550, -500, -450, -400, -350, -300, -250, -200, -150, -100, -50, 50, 100, 150, 200, 250, 300, 350, 400, 450, 500, 550, 600, 700, 800, 900, 1000, 1200, 1500}
		[600] {-1600, -1400, -1200, -1000, -800, -650, -550, -450, -375, -300, -225, -150, -75, 75, 150, 225, 300, 375, 450, 550, 650, 800, 1000, 1200, 1400, 1600}
		[1000] {-1700, -1500, -1300, -1100, -900, -700, -500, -400, -300, -200, -100, 100, 200, 300, 400, 500, 700, 900, 1100, 1300, 1500, 1700}
	U38-N3	[100, 150, 200, 250, 300, 350, 400, 450, 500, 500, 600, 700, 800, 900, 1000, 1200, 1400, 1600, 1800, 2000] {0}
		[200] {-500, -400, -350, -300, -250, -225, -200, -180, -160, -140, -120, -100, -80, -60, -40, -20, 20, 40, 60, 80, 100, 120, 140, 160, 180, 200, 225, 250, 300, 350, 400, 500}
		[400] {-1000, -800, -700, -600, -500, -400, -350, -300, -250, -210, -180, -150, -120, -90, -60, -30, 30, 60, 90, 120, 150, 180, 210, 250, 300, 350, 400, 500, 600, 700, 800, 1000}
		[600] {-1600, -1400, -1200, -1000, -800, -600, -500, -400, -300, -240, -200, -160, -120, -80, -40, 40, 80, 120, 160, 200, 240, 300, 400, 500, 600, 800, 1000, 1200, 1400, 1600}
		[1000] {-3000, -2500, -2000, -1500, -1300, -1100, -900, -700, -600, -500, -400, -300, -200, -100, 100, 200, 300, 400, 500, 600, 700, 900, 1100, 1300, 1500, 2000, 2500, 3000}

Table S10. Spin-lock power and offsets used in the CEST measurements.

construct	Nuclei	**[spin-lock power] {offset frequencies}**
		[ω_1 $2\pi^{-1}$(s^{-1})] {Ω $2\pi^{-1}$(s^{-1})}
TAR (-Mg^{2+})	U23-C6	[10] {-1000.0, -922.2, -844.4, -766.7, -688.9, -611.1, -533.3, -455.6, -377.8, -300.0, -300.0, -289.9, -279.7, -269.6, -259.5, -249.4, -239.2, -229.1, -219.0, -208.9, -198.7, -188.6, -178.5, -168.4, -158.2, -148.1, -138.0, -127.8, -117.7, -107.6, -97.5, -87.3, -77.2, -67.1, -57.0, -46.8, -36.7, -26.6, -16.5, -6.3, 3.8, 13.9, 24.1, 34.2, 44.3, 54.4, 64.6, 74.7, 84.8, 94.9, 105.1, 115.2, 125.3, 135.4, 145.6, 155.7, 165.8, 175.9, 186.1, 196.2, 206.3, 216.5, 226.6, 236.7, 246.8, 257.0, 267.1, 277.2, 287.3, 297.5, 307.6, 317.7, 327.8, 338.0, 348.1, 358.2, 368.4, 378.5, 388.6, 398.7, 408.9, 419.0, 429.1, 439.2, 449.4, 459.5, 469.6, 479.7, 489.9, 500.0, 500.0, 555.6, 611.1, 666.7, 722.2, 777.8, 833.3, 888.9, 944.4, 1000.0}
		[20] {-1000.0, -922.2, -844.4, -766.7, -688.9, -611.1, -533.3, -455.6, -377.8, -300.0, -300.0, -289.9, -279.7, -269.6, -259.5, -249.4, -239.2, -229.1, -219.0, -208.9, -198.7, -188.6, -178.5, -168.4, -158.2, -148.1, -138.0, -127.8, -117.7, -107.6, -97.5, -87.3, -77.2, -67.1, -57.0, -46.8, -36.7, -26.6, -16.5, -6.3, 3.8, 13.9, 24.1, 34.2, 44.3, 54.4, 64.6, 74.7, 84.8, 94.9, 105.1, 115.2, 125.3, 135.4, 145.6, 155.7, 165.8, 175.9, 186.1, 196.2, 206.3, 216.5, 226.6, 236.7, 246.8, 257.0, 267.1, 277.2, 287.3, 297.5, 307.6, 317.7, 327.8, 338.0, 348.1, 358.2, 368.4, 378.5, 388.6, 398.7, 408.9, 419.0, 429.1, 439.2, 449.4, 459.5, 469.6, 479.7, 489.9, 500.0, 500.0, 555.6, 611.1, 666.7, 722.2, 777.8, 833.3, 888.9, 944.4, 1000.0}
		[30] {-1000.0, -922.2, -844.4, -766.7, -688.9, -611.1, -533.3, -455.6, -377.8, -300.0, -300.0, -289.9, -279.7, -269.6, -259.5, -249.4, -239.2, -229.1, -219.0, -208.9, -198.7, -188.6, -178.5, -168.4, -158.2, -148.1, -138.0, -127.8, -117.7, -107.6, -97.5, -87.3, -77.2, -67.1, -57.0, -46.8, -36.7, -26.6, -16.5, -6.3, 3.8, 13.9, 24.1, 34.2, 44.3, 54.4, 64.6, 74.7, 84.8, 94.9, 105.1, 115.2, 125.3, 135.4, 145.6, 155.7, 165.8, 175.9, 186.1, 196.2, 206.3, 216.5, 226.6, 236.7, 246.8, 257.0, 267.1, 277.2, 287.3, 297.5, 307.6, 317.7, 327.8, 338.0, 348.1, 358.2, 368.4, 378.5, 388.6, 398.7, 408.9, 419.0, 429.1, 439.2, 449.4, 459.5, 469.6, 479.7, 489.9, 500.0, 500.0, 555.6, 611.1, 666.7, 722.2, 777.8, 833.3, 888.9, 944.4, 1000.0}
		[40] {-1000.0, -922.2, -844.4, -766.7, -688.9, -611.1, -533.3, -455.6, -377.8, -300.0, -300.0, -289.9, -279.7, -269.6, -259.5, -249.4, -239.2, -229.1, -219.0, -208.9, -198.7, -188.6, -178.5, -168.4, -158.2, -148.1, -138.0, -127.8, -117.7, -107.6, -97.5, -87.3, -77.2, -67.1, -57.0, -46.8, -36.7, -26.6, -16.5, -6.3, 3.8, 13.9, 24.1, 34.2, 44.3, 54.4, 64.6, 74.7, 84.8, 94.9, 105.1, 115.2, 125.3, 135.4, 145.6, 155.7, 165.8, 175.9, 186.1, 196.2, 206.3, 216.5, 226.6, 236.7, 246.8, 257.0, 267.1, 277.2, 287.3, 297.5, 307.6, 317.7, 327.8, 338.0, 348.1, 358.2, 368.4, 378.5, 388.6, 398.7, 408.9, 419.0, 429.1, 439.2, 449.4, 459.5, 469.6, 479.7, 489.9, 500.0, 500.0, 555.6, 611.1, 666.7, 722.2, 777.8, 833.3, 888.9, 944.4, 1000.0}
TAR (-Mg^{2+})	U38-N3	[10] {-800.0, -766.7, -733.3, -700.0, -666.7, -633.3, -600.0, -566.7, -533.3, -500.0, -500.0, -489.9, -479.7, -469.6, -459.5, -449.4, -439.2, -429.1, -419.0, -408.9, -398.7, -388.6, -378.5, -368.4, -358.2, -348.1, -338.0, -327.8, -317.7, -307.6, -297.5, -287.3, -277.2, -267.1, -257.0, -246.8, -236.7, -226.6, -216.5, -206.3, -196.2, -186.1, -175.9, -165.8, -155.7, -145.6, -135.4, -125.3, -115.2, -105.1, -94.9, -84.8, -74.7, -64.6, -54.4, -44.3, -34.2, -24.1, -13.9, -3.8, 6.3, 16.5, 26.6, 36.7, 46.8, 57.0, 67.1, 77.2, 87.3, 97.5, 107.6, 117.7, 127.8, 138.0, 148.1, 158.2, 168.4, 178.5, 188.6, 198.7, 208.9, 219.0, 229.1, 239.2, 249.4, 259.5, 269.6, 279.7, 289.9, 300.0, 300.0, 333.3, 366.7, 400.0, 433.3, 466.7, 500.0, 533.3, 566.7, 600.0}
		[20] {-800.0, -766.7, -733.3, -700.0, -666.7, -633.3, -600.0, -566.7, -533.3, -500.0, -500.0, -489.9, -479.7, -469.6, -459.5, -449.4, -439.2, -429.1, -419.0, -408.9, -398.7, -388.6, -378.5, -368.4, -358.2, -348.1, -338.0, -327.8, -

		317.7, -307.6, -297.5, -287.3, -277.2, -267.1, -257.0, -246.8, -236.7, -226.6, -216.5, -206.3, -196.2, -186.1, -175.9, -165.8, -155.7, -145.6, -135.4, -125.3, -115.2, -105.1, -94.9, -84.8, -74.7, -64.6, -54.4, -44.3, -34.2, -24.1, -13.9, -3.8, 6.3, 16.5, 26.6, 36.7, 46.8, 57.0, 67.1, 77.2, 87.3, 97.5, 107.6, 117.7, 127.8, 138.0, 148.1, 158.2, 168.4, 178.5, 188.6, 198.7, 208.9, 219.0, 229.1, 239.2, 249.4, 259.5, 269.6, 279.7, 289.9, 300.0, 300.0, 333.3, 366.7, 400.0, 433.3, 466.7, 500.0, 533.3, 566.7, 600.0}
		[30] {-800.0, -766.7, -733.3, -700.0, -666.7, -633.3, -600.0, -566.7, -533.3, -500.0, -500.0, -489.9, -479.7, -469.6, -459.5, -449.4, -439.2, -429.1, -419.0, -408.9, -398.7, -388.6, -378.5, -368.4, -358.2, -348.1, -338.0, -327.8, -317.7, -307.6, -297.5, -287.3, -277.2, -267.1, -257.0, -246.8, -236.7, -226.6, -216.5, -206.3, -196.2, -186.1, -175.9, -165.8, -155.7, -145.6, -135.4, -125.3, -115.2, -105.1, -94.9, -84.8, -74.7, -64.6, -54.4, -44.3, -34.2, -24.1, -13.9, -3.8, 6.3, 16.5, 26.6, 36.7, 46.8, 57.0, 67.1, 77.2, 87.3, 97.5, 107.6, 117.7, 127.8, 138.0, 148.1, 158.2, 168.4, 178.5, 188.6, 198.7, 208.9, 219.0, 229.1, 239.2, 249.4, 259.5, 269.6, 279.7, 289.9, 300.0, 300.0, 333.3, 366.7, 400.0, 433.3, 466.7, 500.0, 533.3, 566.7, 600.0}
		[40] {-800.0, -766.7, -733.3, -700.0, -666.7, -633.3, -600.0, -566.7, -533.3, -500.0, -500.0, -489.9, -479.7, -469.6, -459.5, -449.4, -439.2, -429.1, -419.0, -408.9, -398.7, -388.6, -378.5, -368.4, -358.2, -348.1, -338.0, -327.8, -317.7, -307.6, -297.5, -287.3, -277.2, -267.1, -257.0, -246.8, -236.7, -226.6, -216.5, -206.3, -196.2, -186.1, -175.9, -165.8, -155.7, -145.6, -135.4, -125.3, -115.2, -105.1, -94.9, -84.8, -74.7, -64.6, -54.4, -44.3, -34.2, -24.1, -13.9, -3.8, 6.3, 16.5, 26.6, 36.7, 46.8, 57.0, 67.1, 77.2, 87.3, 97.5, 107.6, 117.7, 127.8, 138.0, 148.1, 158.2, 168.4, 178.5, 188.6, 198.7, 208.9, 219.0, 229.1, 239.2, 249.4, 259.5, 269.6, 279.7, 289.9, 300.0, 300.0, 333.3, 366.7, 400.0, 433.3, 466.7, 500.0, 533.3, 566.7, 600.0}
		[50] {-800.0, -766.7, -733.3, -700.0, -666.7, -633.3, -600.0, -566.7, -533.3, -500.0, -500.0, -489.9, -479.7, -469.6, -459.5, -449.4, -439.2, -429.1, -419.0, -408.9, -398.7, -388.6, -378.5, -368.4, -358.2, -348.1, -338.0, -327.8, -317.7, -307.6, -297.5, -287.3, -277.2, -267.1, -257.0, -246.8, -236.7, -226.6, -216.5, -206.3, -196.2, -186.1, -175.9, -165.8, -155.7, -145.6, -135.4, -125.3, -115.2, -105.1, -94.9, -84.8, -74.7, -64.6, -54.4, -44.3, -34.2, -24.1, -13.9, -3.8, 6.3, 16.5, 26.6, 36.7, 46.8, 57.0, 67.1, 77.2, 87.3, 97.5, 107.6, 117.7, 127.8, 138.0, 148.1, 158.2, 168.4, 178.5, 188.6, 198.7, 208.9, 219.0, 229.1, 239.2, 249.4, 259.5, 269.6, 279.7, 289.9, 300.0, 300.0, 333.3, 366.7, 400.0, 433.3, 466.7, 500.0, 533.3, 566.7, 600.0}
TAR-C24U25A35 (-Mg^{2+})	U23-C6	[5] {-1000.0, -922.2, -844.4, -766.7, -688.9, -611.1, -533.3, -455.6, -377.8, -300.0, -300.0, -289.9, -279.7, -269.6, -259.5, -249.4, -239.2, -229.1, -219.0, -208.9, -198.7, -188.6, -178.5, -168.4, -158.2, -148.1, -138.0, -127.8, -117.7, -107.6, -97.5, -87.3, -77.2, -67.1, -57.0, -46.8, -36.7, -26.6, -16.5, -6.3, 3.8, 13.9, 24.1, 34.2, 44.3, 54.4, 64.6, 74.7, 84.8, 94.9, 105.1, 115.2, 125.3, 135.4, 145.6, 155.7, 165.8, 175.9, 186.1, 196.2, 206.3, 216.5, 226.6, 236.7, 246.8, 257.0, 267.1, 277.2, 287.3, 297.5, 307.6, 317.7, 327.8, 338.0, 348.1, 358.2, 368.4, 378.5, 388.6, 398.7, 408.9, 419.0, 429.1, 439.2, 449.4, 459.5, 469.6, 479.7, 489.9, 500.0, 500.0, 555.6, 611.1, 666.7, 722.2, 777.8, 833.3, 888.9, 944.4, 1000.0}
		[10] {-1000.0, -922.2, -844.4, -766.7, -688.9, -611.1, -533.3, -455.6, -377.8, -300.0, -300.0, -289.9, -279.7, -269.6, -259.5, -249.4, -239.2, -229.1, -219.0, -208.9, -198.7, -188.6, -178.5, -168.4, -158.2, -148.1, -138.0, -127.8, -117.7, -107.6, -97.5, -87.3, -77.2, -67.1, -57.0, -46.8, -36.7, -26.6, -16.5, -6.3, 3.8, 13.9, 24.1, 34.2, 44.3, 54.4, 64.6, 74.7, 84.8, 94.9, 105.1, 115.2, 125.3, 135.4, 145.6, 155.7, 165.8, 175.9, 186.1, 196.2, 206.3, 216.5, 226.6, 236.7, 246.8, 257.0, 267.1, 277.2, 287.3, 297.5, 307.6, 317.7, 327.8, 338.0, 348.1, 358.2, 368.4, 378.5, 388.6, 398.7, 408.9, 419.0, 429.1, 439.2, 449.4, 459.5, 469.6, 479.7, 489.9, 500.0, 500.0, 555.6, 611.1, 666.7, 722.2, 777.8, 833.3, 888.9, 944.4, 1000.0}

		[25] {-1000.0, -922.2, -844.4, -766.7, -688.9, -611.1, -533.3, -455.6, -377.8, -300.0, -300.0, -289.9, -279.7, -269.6, -259.5, -249.4, -239.2, -229.1, -219.0, -208.9, -198.7, -188.6, -178.5, -168.4, -158.2, -148.1, -138.0, -127.8, -117.7, -107.6, -97.5, -87.3, -77.2, -67.1, -57.0, -46.8, -36.7, -26.6, -16.5, -6.3, 3.8, 13.9, 24.1, 34.2, 44.3, 54.4, 64.6, 74.7, 84.8, 94.9, 105.1, 115.2, 125.3, 135.4, 145.6, 155.7, 165.8, 175.9, 186.1, 196.2, 206.3, 216.5, 226.6, 236.7, 246.8, 257.0, 267.1, 277.2, 287.3, 297.5, 307.6, 317.7, 327.8, 338.0, 348.1, 358.2, 368.4, 378.5, 388.6, 398.7, 408.9, 419.0, 429.1, 439.2, 449.4, 459.5, 469.6, 479.7, 489.9, 500.0, 500.0, 555.6, 611.1, 666.7, 722.2, 777.8, 833.3, 888.9, 944.4, 1000.0}
		[50] {-1000.0, -922.2, -844.4, -766.7, -688.9, -611.1, -533.3, -455.6, -377.8, -300.0, -300.0, -289.9, -279.7, -269.6, -259.5, -249.4, -239.2, -229.1, -219.0, -208.9, -198.7, -188.6, -178.5, -168.4, -158.2, -148.1, -138.0, -127.8, -117.7, -107.6, -97.5, -87.3, -77.2, -67.1, -57.0, -46.8, -36.7, -26.6, -16.5, -6.3, 3.8, 13.9, 24.1, 34.2, 44.3, 54.4, 64.6, 74.7, 84.8, 94.9, 105.1, 115.2, 125.3, 135.4, 145.6, 155.7, 165.8, 175.9, 186.1, 196.2, 206.3, 216.5, 226.6, 236.7, 246.8, 257.0, 267.1, 277.2, 287.3, 297.5, 307.6, 317.7, 327.8, 338.0, 348.1, 358.2, 368.4, 378.5, 388.6, 398.7, 408.9, 419.0, 429.1, 439.2, 449.4, 459.5, 469.6, 479.7, 489.9, 500.0, 500.0, 555.6, 611.1, 666.7, 722.2, 777.8, 833.3, 888.9, 944.4, 1000.0}
TAR-C24U25A35 (-Mg^{2+})	U38-N3	[10] {-1000.0, -944.4, -888.9, -833.3, -777.8, -722.2, -666.7, -611.1, -555.6, -500.0, -500.0, -489.9, -479.7, -469.6, -459.5, -449.4, -439.2, -429.1, -419.0, -408.9, -398.7, -388.6, -378.5, -368.4, -358.2, -348.1, -338.0, -327.8, -317.7, -307.6, -297.5, -287.3, -277.2, -267.1, -257.0, -246.8, -236.7, -226.6, -216.5, -206.3, -196.2, -186.1, -175.9, -165.8, -155.7, -145.6, -135.4, -125.3, -115.2, -105.1, -94.9, -84.8, -74.7, -64.6, -54.4, -44.3, -34.2, -24.1, -13.9, -3.8, 6.3, 16.5, 26.6, 36.7, 46.8, 57.0, 67.1, 77.2, 87.3, 97.5, 107.6, 117.7, 127.8, 138.0, 148.1, 158.2, 168.4, 178.5, 188.6, 198.7, 208.9, 219.0, 229.1, 239.2, 249.4, 259.5, 269.6, 279.7, 289.9, 300.0, 300.0, 377.8, 455.6, 533.3, 611.1, 688.9, 766.7, 844.4, 922.2, 1000.0}
		[20] {-1000.0, -944.4, -888.9, -833.3, -777.8, -722.2, -666.7, -611.1, -555.6, -500.0, -500.0, -489.9, -479.7, -469.6, -459.5, -449.4, -439.2, -429.1, -419.0, -408.9, -398.7, -388.6, -378.5, -368.4, -358.2, -348.1, -338.0, -327.8, -317.7, -307.6, -297.5, -287.3, -277.2, -267.1, -257.0, -246.8, -236.7, -226.6, -216.5, -206.3, -196.2, -186.1, -175.9, -165.8, -155.7, -145.6, -135.4, -125.3, -115.2, -105.1, -94.9, -84.8, -74.7, -64.6, -54.4, -44.3, -34.2, -24.1, -13.9, -3.8, 6.3, 16.5, 26.6, 36.7, 46.8, 57.0, 67.1, 77.2, 87.3, 97.5, 107.6, 117.7, 127.8, 138.0, 148.1, 158.2, 168.4, 178.5, 188.6, 198.7, 208.9, 219.0, 229.1, 239.2, 249.4, 259.5, 269.6, 279.7, 289.9, 300.0, 300.0, 377.8, 455.6, 533.3, 611.1, 688.9, 766.7, 844.4, 922.2, 1000.0}
		[25] {-1000.0, -944.4, -888.9, -833.3, -777.8, -722.2, -666.7, -611.1, -555.6, -500.0, -500.0, -489.9, -479.7, -469.6, -459.5, -449.4, -439.2, -429.1, -419.0, -408.9, -398.7, -388.6, -378.5, -368.4, -358.2, -348.1, -338.0, -327.8, -317.7, -307.6, -297.5, -287.3, -277.2, -267.1, -257.0, -246.8, -236.7, -226.6, -216.5, -206.3, -196.2, -186.1, -175.9, -165.8, -155.7, -145.6, -135.4, -125.3, -115.2, -105.1, -94.9, -84.8, -74.7, -64.6, -54.4, -44.3, -34.2, -24.1, -13.9, -3.8, 6.3, 16.5, 26.6, 36.7, 46.8, 57.0, 67.1, 77.2, 87.3, 97.5, 107.6, 117.7, 127.8, 138.0, 148.1, 158.2, 168.4, 178.5, 188.6, 198.7, 208.9, 219.0, 229.1, 239.2, 249.4, 259.5, 269.6, 279.7, 289.9, 300.0, 300.0, 377.8, 455.6, 533.3, 611.1, 688.9, 766.7, 844.4, 922.2, 1000.0}
		[30] {-1000.0, -944.4, -888.9, -833.3, -777.8, -722.2, -666.7, -611.1, -555.6, -500.0, -500.0, -489.9, -479.7, -469.6, -459.5, -449.4, -439.2, -429.1, -419.0, -408.9, -398.7, -388.6, -378.5, -368.4, -358.2, -348.1, -338.0, -327.8, -317.7, -307.6, -297.5, -287.3, -277.2, -267.1, -257.0, -246.8, -236.7, -226.6, -216.5, -206.3, -196.2, -186.1, -175.9, -165.8, -155.7, -145.6, -135.4, -125.3, -115.2, -105.1, -94.9, -84.8, -74.7, -64.6, -54.4, -44.3, -34.2, -24.1, -13.9, -3.8, 6.3, 16.5, 26.6, 36.7, 46.8, 57.0, 67.1, 77.2, 87.3, 97.5, 107.6, 117.7, 127.8, 138.0, 148.1,

		158.2, 168.4, 178.5, 188.6, 198.7, 208.9, 219.0, 229.1, 239.2, 249.4, 259.5, 269.6, 279.7, 289.9, 300.0, 300.0, 377.8, 455.6, 533.3, 611.1, 688.9, 766.7, 844.4, 922.2, 1000.0}
TAR-C24U25A35 (+Mg^{2+})	U23-C6	[10] {-1000.0, -922.2, -844.4, -766.7, -688.9, -611.1, -533.3, -455.6, -377.8, -300.0, -300.0, -289.9, -279.7, -269.6, -259.5, -249.4, -239.2, -229.1, -219.0, -208.9, -198.7, -188.6, -178.5, -168.4, -158.2, -148.1, -138.0, -127.8, -117.7, -107.6, -97.5, -87.3, -77.2, -67.1, -57.0, -46.8, -36.7, -26.6, -16.5, -6.3, 3.8, 13.9, 24.1, 34.2, 44.3, 54.4, 64.6, 74.7, 84.8, 94.9, 105.1, 115.2, 125.3, 135.4, 145.6, 155.7, 165.8, 175.9, 186.1, 196.2, 206.3, 216.5, 226.6, 236.7, 246.8, 257.0, 267.1, 277.2, 287.3, 297.5, 307.6, 317.7, 327.8, 338.0, 348.1, 358.2, 368.4, 378.5, 388.6, 398.7, 408.9, 419.0, 429.1, 439.2, 449.4, 459.5, 469.6, 479.7, 489.9, 500.0, 500.0, 555.6, 611.1, 666.7, 722.2, 777.8, 833.3, 888.9, 944.4, 1000.0}
		[20] {-1000.0, -922.2, -844.4, -766.7, -688.9, -611.1, -533.3, -455.6, -377.8, -300.0, -300.0, -289.9, -279.7, -269.6, -259.5, -249.4, -239.2, -229.1, -219.0, -208.9, -198.7, -188.6, -178.5, -168.4, -158.2, -148.1, -138.0, -127.8, -117.7, -107.6, -97.5, -87.3, -77.2, -67.1, -57.0, -46.8, -36.7, -26.6, -16.5, -6.3, 3.8, 13.9, 24.1, 34.2, 44.3, 54.4, 64.6, 74.7, 84.8, 94.9, 105.1, 115.2, 125.3, 135.4, 145.6, 155.7, 165.8, 175.9, 186.1, 196.2, 206.3, 216.5, 226.6, 236.7, 246.8, 257.0, 267.1, 277.2, 287.3, 297.5, 307.6, 317.7, 327.8, 338.0, 348.1, 358.2, 368.4, 378.5, 388.6, 398.7, 408.9, 419.0, 429.1, 439.2, 449.4, 459.5, 469.6, 479.7, 489.9, 500.0, 500.0, 555.6, 611.1, 666.7, 722.2, 777.8, 833.3, 888.9, 944.4, 1000.0}
		[30] {-1000.0, -922.2, -844.4, -766.7, -688.9, -611.1, -533.3, -455.6, -377.8, -300.0, -300.0, -289.9, -279.7, -269.6, -259.5, -249.4, -239.2, -229.1, -219.0, -208.9, -198.7, -188.6, -178.5, -168.4, -158.2, -148.1, -138.0, -127.8, -117.7, -107.6, -97.5, -87.3, -77.2, -67.1, -57.0, -46.8, -36.7, -26.6, -16.5, -6.3, 3.8, 13.9, 24.1, 34.2, 44.3, 54.4, 64.6, 74.7, 84.8, 94.9, 105.1, 115.2, 125.3, 135.4, 145.6, 155.7, 165.8, 175.9, 186.1, 196.2, 206.3, 216.5, 226.6, 236.7, 246.8, 257.0, 267.1, 277.2, 287.3, 297.5, 307.6, 317.7, 327.8, 338.0, 348.1, 358.2, 368.4, 378.5, 388.6, 398.7, 408.9, 419.0, 429.1, 439.2, 449.4, 459.5, 469.6, 479.7, 489.9, 500.0, 500.0, 555.6, 611.1, 666.7, 722.2, 777.8, 833.3, 888.9, 944.4, 1000.0}
		[40] {-1000.0, -922.2, -844.4, -766.7, -688.9, -611.1, -533.3, -455.6, -377.8, -300.0, -300.0, -289.9, -279.7, -269.6, -259.5, -249.4, -239.2, -229.1, -219.0, -208.9, -198.7, -188.6, -178.5, -168.4, -158.2, -148.1, -138.0, -127.8, -117.7, -107.6, -97.5, -87.3, -77.2, -67.1, -57.0, -46.8, -36.7, -26.6, -16.5, -6.3, 3.8, 13.9, 24.1, 34.2, 44.3, 54.4, 64.6, 74.7, 84.8, 94.9, 105.1, 115.2, 125.3, 135.4, 145.6, 155.7, 165.8, 175.9, 186.1, 196.2, 206.3, 216.5, 226.6, 236.7, 246.8, 257.0, 267.1, 277.2, 287.3, 297.5, 307.6, 317.7, 327.8, 338.0, 348.1, 358.2, 368.4, 378.5, 388.6, 398.7, 408.9, 419.0, 429.1, 439.2, 449.4, 459.5, 469.6, 479.7, 489.9, 500.0, 500.0, 555.6, 611.1, 666.7, 722.2, 777.8, 833.3, 888.9, 944.4, 1000.0}
	U38-N3	[10] {-1000.0, -944.4, -888.9, -833.3, -777.8, -722.2, -666.7, -611.1, -555.6, -500.0, -500.0, -489.9, -479.7, -469.6, -459.5, -449.4, -439.2, -429.1, -419.0, -408.9, -398.7, -388.6, -378.5, -368.4, -358.2, -348.1, -338.0, -327.8, -317.7, -307.6, -297.5, -287.3, -277.2, -267.1, -257.0, -246.8, -236.7, -226.6, -216.5, -206.3, -196.2, -186.1, -175.9, -165.8, -155.7, -145.6, -135.4, -125.3, -115.2, -105.1, -94.9, -84.8, -74.7, -64.6, -54.4, -44.3, -34.2, -24.1, -13.9, -3.8, 6.3, 16.5, 26.6, 36.7, 46.8, 57.0, 67.1, 77.2, 87.3, 97.5, 107.6, 117.7, 127.8, 138.0, 148.1, 158.2, 168.4, 178.5, 188.6, 198.7, 208.9, 219.0, 229.1, 239.2, 249.4, 259.5, 269.6, 279.7, 289.9, 300.0, 300.0, 377.8, 455.6, 533.3, 611.1, 688.9, 766.7, 844.4, 922.2, 1000.0}
TAR-C24U25A35 (+Mg^{2+})		[20] {-1000.0, -944.4, -888.9, -833.3, -777.8, -722.2, -666.7, -611.1, -555.6, -500.0, -500.0, -489.9, -479.7, -469.6, -459.5, -449.4, -439.2, -429.1, -419.0, -408.9, -398.7, -388.6, -378.5, -368.4, -358.2, -348.1, -338.0, -327.8, -317.7, -307.6, -297.5, -287.3, -277.2, -267.1, -257.0, -246.8, -236.7, -226.6, -216.5, -206.3, -196.2, -186.1, -175.9, -165.8, -155.7, -145.6, -135.4, -125.3, -115.2, -105.1, -94.9, -84.8, -74.7, -64.6, -54.4, -44.3, -34.2,

		-24.1, -13.9, -3.8, 6.3, 16.5, 26.6, 36.7, 46.8, 57.0, 67.1, 77.2, 87.3, 97.5, 107.6, 117.7, 127.8, 138.0, 148.1, 158.2, 168.4, 178.5, 188.6, 198.7, 208.9, 219.0, 229.1, 239.2, 249.4, 259.5, 269.6, 279.7, 289.9, 300.0, 300.0, 377.8, 455.6, 533.3, 611.1, 688.9, 766.7, 844.4, 922.2, 1000.0}
		[30] {-1000.0, -944.4, -888.9, -833.3, -777.8, -722.2, -666.7, -611.1, -555.6, -500.0, -500.0, -489.9, -479.7, -469.6, -459.5, -449.4, -439.2, -429.1, -419.0, -408.9, -398.7, -388.6, -378.5, -368.4, -358.2, -348.1, -338.0, -327.8, -317.7, -307.6, -297.5, -287.3, -277.2, -267.1, -257.0, -246.8, -236.7, -226.6, -216.5, -206.3, -196.2, -186.1, -175.9, -165.8, -155.7, -145.6, -135.4, -125.3, -115.2, -105.1, -94.9, -84.8, -74.7, -64.6, -54.4, -44.3, -34.2, -24.1, -13.9, -3.8, 6.3, 16.5, 26.6, 36.7, 46.8, 57.0, 67.1, 77.2, 87.3, 97.5, 107.6, 117.7, 127.8, 138.0, 148.1, 158.2, 168.4, 178.5, 188.6, 198.7, 208.9, 219.0, 229.1, 239.2, 249.4, 259.5, 269.6, 279.7, 289.9, 300.0, 300.0, 377.8, 455.6, 533.3, 611.1, 688.9, 766.7, 844.4, 922.2, 1000.0}
		[40] {-1000.0, -944.4, -888.9, -833.3, -777.8, -722.2, -666.7, -611.1, -555.6, -500.0, -500.0, -489.9, -479.7, -469.6, -459.5, -449.4, -439.2, -429.1, -419.0, -408.9, -398.7, -388.6, -378.5, -368.4, -358.2, -348.1, -338.0, -327.8, -317.7, -307.6, -297.5, -287.3, -277.2, -267.1, -257.0, -246.8, -236.7, -226.6, -216.5, -206.3, -196.2, -186.1, -175.9, -165.8, -155.7, -145.6, -135.4, -125.3, -115.2, -105.1, -94.9, -84.8, -74.7, -64.6, -54.4, -44.3, -34.2, -24.1, -13.9, -3.8, 6.3, 16.5, 26.6, 36.7, 46.8, 57.0, 67.1, 77.2, 87.3, 97.5, 107.6, 117.7, 127.8, 138.0, 148.1, 158.2, 168.4, 178.5, 188.6, 198.7, 208.9, 219.0, 229.1, 239.2, 249.4, 259.5, 269.6, 279.7, 289.9, 300.0, 300.0, 377.8, 455.6, 533.3, 611.1, 688.9, 766.7, 844.4, 922.2, 1000.0}

Reference

1. Dethoff, E.A., Petzold, K., Chugh, J., Casiano-Negroni, A. and Al-Hashimi, H.M. (2012) Visualizing transient low-populated structures of RNA. *Nature*, **491**, 724-728.
2. Kimsey, I.J., Petzold, K., Sathyamoorthy, B., Stein, Z.W. and Al-Hashimi, H.M. (2015) Visualizing transient Watson-Crick-like mispairs in DNA and RNA duplexes. *Nature*, **519**, 315-320.
3. Lee, J., Dethoff, E.A. and Al-Hashimi, H.M. (2014) Invisible RNA state dynamically couples distant motifs. *Proc Natl Acad Sci*, **111**, 9485-9490.